NJC

Cite this: *New J. Chem.*, 2011, **35**, 587–601

www.rsc.org/njc

PAPER

De novo synthesis and photophysical characterization of annulated bacteriochlorins. Mimicking and extending the properties of bacteriochlorophylls†

Michael Krayer,[a] Eunkyung Yang,[b] James R. Diers,[c] David F. Bocian,*[c] Dewey Holten*[b] and Jonathan S. Lindsey*[a]

Received (in Montpellier, France) 8th October 2010, Accepted 22nd November 2010
DOI: 10.1039/c0nj00771d

Bacteriochlorophylls contain the bacteriochlorin chromophore and a fifth, five-membered oxopentano ring that encompasses positions 13–15 known as the "isocyclic" ring E. Such bacterio-13[1]-oxophorbines have heretofore only been available in the naturally occurring compounds, and analogues bearing six-membered rings have only been available by derivatization of bacteriochlorophylls. A *de novo* route to synthetic bacteriochlorins, which bear a geminal dimethyl group in each pyrroline ring, has been extended to gain access to a bacterio-13[1]-oxophorbine and bacteriochlorin-13,15-dicarboximides. The route relies on acid-catalyzed condensation of a dihydrodipyrrin-acetal to form the bacteriochlorin, which then is subjected to regioselective 15-bromination. Pd-mediated cyclization of the 15-bromobacteriochlorin bearing a 13-acetyl group (intramolecular α-arylation) or 13-ethoxycarbonyl group (carbamoylation and intramolecular imidation) gives the bacterio-13[1]-oxophorbine or bacteriochlorin-13,15-dicarboximide, respectively. The resulting macrocycles exhibit absorption in the near-infrared spectral region (733–818 nm), which extends the spectral coverage beyond that obtained previously with synthetic bacteriochlorins that lack a fifth ring. The macrocycles also exhibit excited singlet-state lifetimes (1.9–4.6 ns) comparable to or longer than those of natural photosynthetic pigments. Density functional theory calculations predict that the bathochromically shifted absorption is primarily due to lowering of the energy of the lowest unoccupied molecular orbital. The new route complements existing semisynthetic routes and should enable fundamental spectroscopic studies and diverse photochemical applications.

Introduction

Bacteriochlorins absorb strongly in the near-infrared spectral region[1] and hence are attractive candidates for a wide variety of photochemical studies, including artificial photosynthesis,[2–9] photodynamic therapy (PDT),[10–23] optical imaging,[24–26] and perhaps flow cytometry.[24,27] Naturally occurring bacteriochlorophylls *a*, *b*, and *g* contain the bacteriochlorin chromophore and provide the basis for light-harvesting processes and electron-transfer reactions in bacterial photosynthesis (Chart 1, panel A).[28] Bacteriochlorophylls also possess a five-membered ring (ring E) that encompasses the 13- and 15-positions; the ring contains a 13[1]-oxo moiety and a 13[2]-methoxycarbonyl substituent. Synthetic manipulation of bacteriochlorophylls has afforded a number of derivatives including (i) bacteriopyropheophorbides, which lack the 13[2]-methoxycarbonyl substituent, the phytyl-like chain, and the central magnesium;[2–4,29,30] and (ii) bacteriopurpurinimides (hereafter referred to as bacteriochlorin-imides), which bear a six-membered imide ring (Chart 1, panel B).[6,12,16,17,31–37]

The presence of the imide ring in bacteriochlorin-imides provides a number of attractions including (1) a hyperchromic and bathochromic shift of the long-wavelength absorption band; (2) the ability to introduce diverse groups at the nitrogen of the imide ring;[38] and (3) increased stability of the macrocycle toward routine handling due to the presence of the second carbonyl group at the 15-position. So far, bacteriochlorins bearing the five membered oxopentano or six-membered imide ring have only been available from the natural compounds or upon semisynthesis therefrom, respectively, although synthetic porphyrins and chlorins with a wide variety of annulated rings have been prepared.[39,40] Two significant problems in the preparation of derivatives of bacteriochlorophylls include

[a] *Department of Chemistry, North Carolina State University, Raleigh, North Carolina, 27695-8204, USA. E-mail: jlindsey@ncsu.edu*
[b] *Department of Chemistry, Washington University, St. Louis, Missouri, 63130-4889, USA. E-mail: holten@wustl.edu*
[c] *Department of Chemistry, University of California, Riverside, California, 92521-0403, USA. E-mail: David.Bocian@ucr.edu*
† Electronic supplementary information (ESI) available: Spectral data for all new compounds. See DOI: 10.1039/c0nj00771d

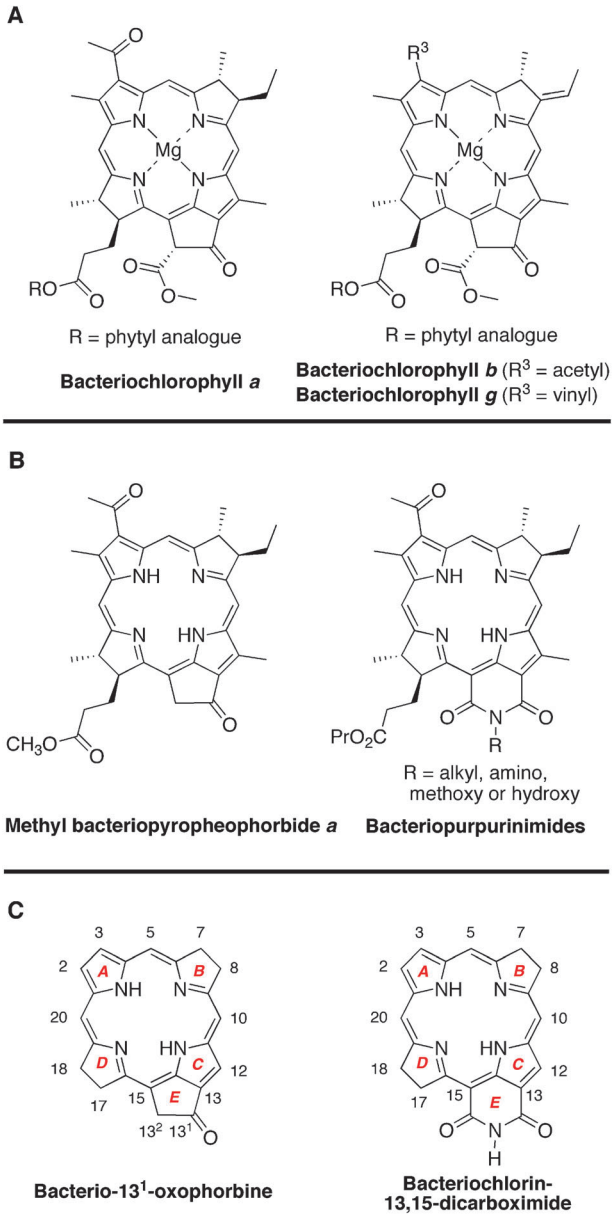

Chart 1 (A) Naturally occurring bacteriochlorophylls. (B) Derivatives of naturally occurring bacteriochlorophylls. (C) Nomenclature of the core macrocycles.

limited stability[36,41,42] and poor synthetic malleability owing to the presence of a nearly full complement of substituents about the perimeter of the macrocycle.[13,18] The synthesis of bacteriochlorins by reduction or addition of porphyrins or chlorins is appropriate for a number of applications but generally suffers from a lack of regiocontrol.[43]

Over the past decade we have been developing a *de novo* synthesis of bacteriochlorins.[44–46] The route affords bacteriochlorins wherein each pyrroline ring contains a geminal dimethyl group rather than the *trans*-dialkyl and *exo*-ethylidene moieties of the naturally occurring bacteriochlorophylls. The geminal dimethyl group has the attractive feature of stabilizing the macrocycle toward adventitious dehydrogenation. Synthetic bacteriochlorins bearing diverse substituents at specific sites in the pyrrolic units have been prepared, and selected derivatization processes of the bacteriochlorins have been examined (including regioselective bromination); however, no annulated rings have yet been introduced.[44–51] Here we extend the *de novo* route to create stable, tailorable analogues of the fundamental bacterio-13¹-oxophorbine and bacteriochlorin-13,15-dicarboximide macrocyclic skeletons (Chart 1, panel C).[52] The synthesis and spectroscopic analysis of such synthetic macrocycles is essential for understanding the structural features that underpin the characteristic spectral properties of the naturally occurring bacteriochlorophylls.

Results and discussion

I Retrosynthetic analysis

An approach to stable bacterio-13¹-oxophorbine and bacteriochlorin-13,15-dicarboximide macrocycles is outlined in Scheme 1. The bacteriochlorin macrocycle is created upon acid-catalyzed condensation of a dihydrodipyrrin-acetal. Subsequent derivatization to install the annulated rings builds

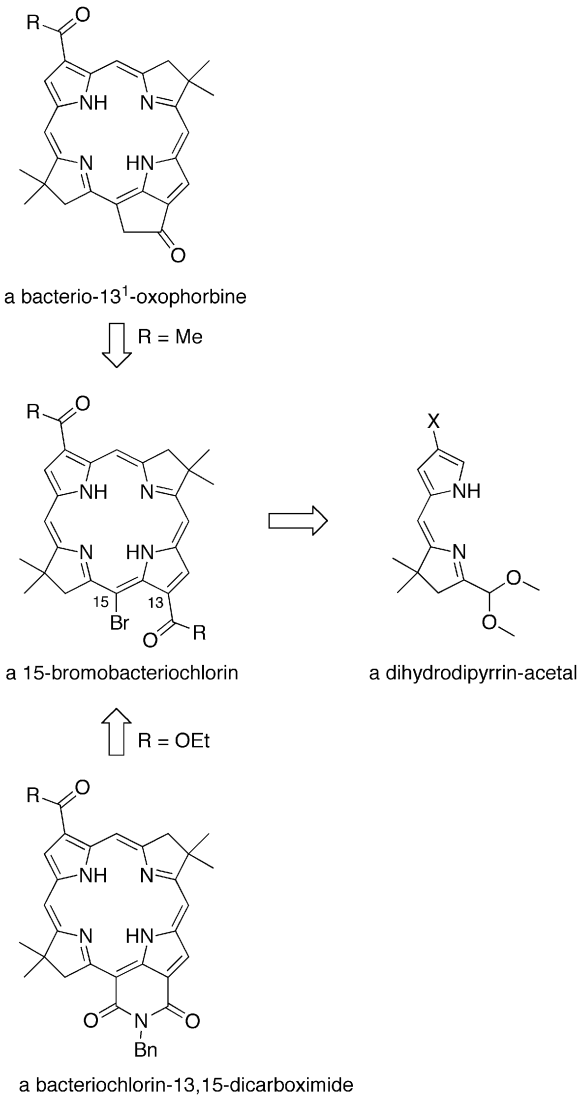

Scheme 1 Retrosynthetic analysis of stable synthetic bacteriochlorins containing a fifth ring.

on the strategies we have developed in chlorin chemistry for the preparation of the 13[1]-oxophorbine[53] and chlorin-imide[54] frameworks. Thus, the construction of both rings relies on regioselective 15-bromination followed by intramolecular Pd-mediated ring closure. Access to the former requires the presence of a 13-acetyl group for α-arylation[55] whereas the latter requires a 13-ester group for carbonylation and imidation.

II Regioselective 15-bromination

A number of 5-methoxy substituted bacteriochlorins are known to undergo regioselective 15-bromination.[46,47] Therefore, an initial approach to the target bacteriochlorin-13[1]-oxophorbine was to convert the 3,13-dibromo-5-methoxybacteriochlorin **MeOBC-Br** to the 3,13-diacetyl-5-methoxybacteriochlorin **MeOBC-A** followed by 15-bromination and Pd-mediated ring closure. However, the presence of 3,13-diacetyl groups in **MeOBC-A** caused loss of regioselectivity during the bromination step (Scheme 2). This result was not entirely surprising, given that the same loss of regioselectivity was observed in the case of a bacteriochlorin bearing 3,13-diester groups.[46] **MeOBC-A** was treated with ethylene glycol and TMSCl[56] to form the ketal-protected analogue **MeOBC-K** in an attempt to mitigate the electron-withdrawing effect of the acetyl group, but again regioselective bromination was not obtained (Scheme 2).

To effect regioselective 15-bromination in the presence of electron-withdrawing substituents (*e.g.*, acetyl or ester), the remaining β-pyrrolic positions need to be blocked, which can be achieved with alkyl groups. Indeed, we have previously reported the regioselective bromination of 2,12-diethyl-3,13-diethoxycarbonyl-5-methoxybacteriochlorin **MeOBC-EtEs** to give the key precursor to the bacteriochlorin-13,15-dicarboximides, the 15-bromobacteriochlorin **MeOBC-EtEs-Br**[15] (Scheme 3).[46] The use of bacteriochlorins wherein the three β-pyrrolic sites that are not integral to ring E are substituted (*i.e.*, positions 2, 3, and 12) proved to be an essential requirement for the approaches developed here to introduce the two ring E motifs.

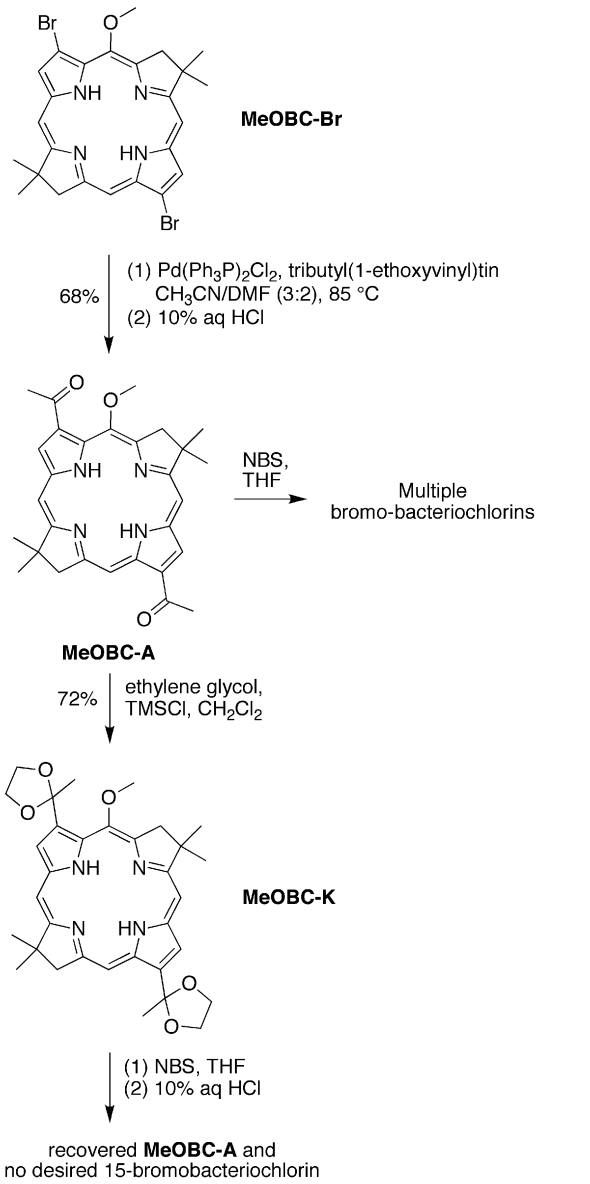

Scheme 2 Attempted synthesis of a 15-bromo-3,13-diacetyl-bacteriochlorin.

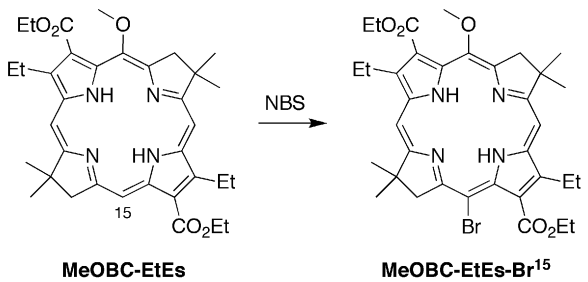

Scheme 3 Prior demonstration of regioselective 15-bromination.

III Synthesis

The target bacterio-13[1]-oxophorbine was pursued *via* the intermediacy of dihydrodipyrrin-acetal **1**, which bears bromo and methyl substituents at the β-pyrrolic positions (Scheme 4). Upon conversion to the bacteriochlorin, the bromo substituent provides a synthetic handle for introduction of the acetyl group, and the methyl group prevents bromination at the pyrrolic positions during 15-bromination. Preparation of **1** closely follows the optimized condition for a dihydrodipyrrin-acetal lacking the methyl group on the pyrrole.[50] The synthesis of **1** entails formation of 3-methyl-pyrrole-2-carboxaldehyde (**2**) by photochemical rearrangement of 4-picoline-*N*-oxide,[57] bromination to give bromopyrrole **3**, tosyl-protection of the pyrrole (**3-Ts**), nitro-aldol (Henry) condensation followed by reduction to give the 2-(2-nitroethyl)pyrrole **4-Ts**, Michael addition with the α,β-unsaturated ketone-acetal **5**[44] to give the nitrohexanone-pyrrole **6-Ts**, removal of the tosyl group (**6-H**), and McMurry-type ring closure to **1**. The presence of the tosyl group was necessary to increase the stability of key intermediates.

Dihydrodipyrrin-acetal **1** was subjected to self-condensation conditions optimized for selective formation of either the

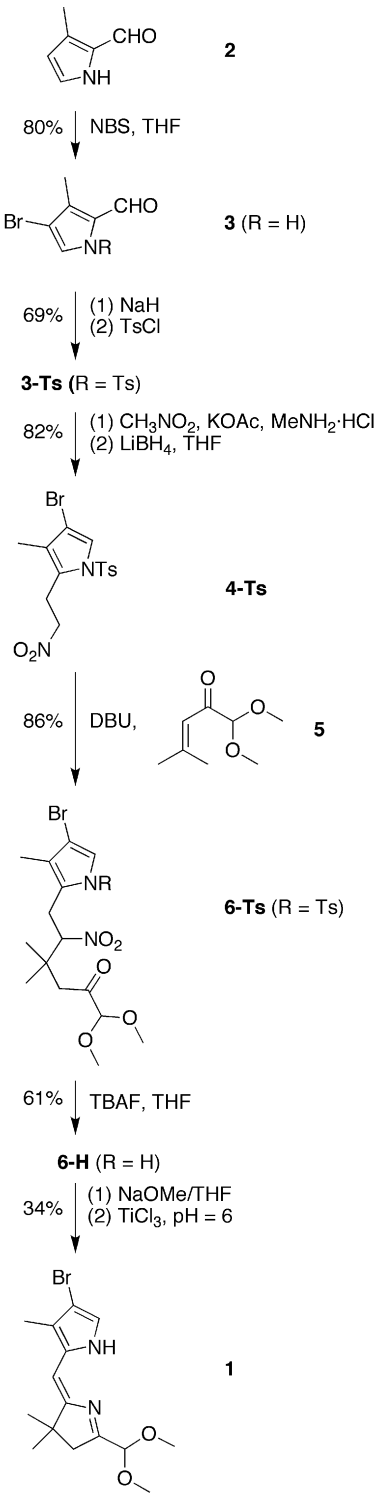

Scheme 4 Synthesis of a bromo-dihydrodipyrrin-acetal.

5-methoxybacteriochlorin or the 5-unsubstituted-bacteriochlorin.[44,46] Thus, self-condensation of **1** in CH_2Cl_2 containing TMSOTf/2,6-DTBP gave **MeOBC-MeBr**; self-condensation in CH_3CN containing $BF_3{\cdot}OEt_2$ gave **HBC-MeBr**. Stille coupling of each bacteriochlorin with tributyl(1-ethoxyvinyl)tin[58] followed by acidic hydrolysis gave diacetylbacteriochlorins **MeOBC-MeA** and **HBC-MeA**. (Note: the reactions were carried out in THF for 23 h[45] instead of DMF/CH_3CN[59] for 2 h; the latter afforded mono-reacted bromo-acetylbacteriochlorin.) 15-Bromination of 5-methoxybacteriochlorin **MeOBC-MeA** proceeded smoothly to give **MeOBC-MeA-Br**[15], whereas treatment of 5-unsubstituted-bacteriochlorin **HBC-MeA** with 1 equiv. of NBS gave the 5,15-dibromobacteriochlorin **BC-MeA-Br**[5,15] as the major product. Nonetheless, Pd-mediated intramolecular α-arylation of **MeOBC-MeA-Br**[15] created ring E and thereby completed the synthesis of the 5-methoxybacterio-13^1-oxophorbine **MeOBOP** (Scheme 5). Attempted double cyclization of **BC-MeA-Br**[5,15] to give the bacteriochlorin-3^1,13^1-dioxophorbine was unsuccessful.

For the synthesis of bacteriochlorin-13,15-dicarboximides, the known diester-bacteriochlorins[46] **MeOBC-EtEs** and **HBC-EtEs** were subjected to bromination. As before (Scheme 3), the bromination of 5-methoxybacteriochlorin **MeOBC-EtEs** proceeded smoothly to give the 15-bromo-bacteriochlorin **MeOBC-EtEs-Br**[15].[46] On the other hand, **HBC-EtEs** gave predominantly the 5,15-dibrominated product; however, the mono-brominated **HBC-EtEs-Br**[15] was isolated in sufficient quantities to complete the synthesis. Treatment of **MeOBC-EtEs-Br**[15] or **HBC-EtEs-Br**[15] in the presence of benzylamine to one-flask Pd-mediated carbamoylation and ring closure resulted in the bacteriochlorin-13,15-dicarboximide **MeOBC-I** or **HBC-I**, respectively (Scheme 6).

IV Structural characterization

The bacteriochlorins were characterized by ^{1}H NMR spectroscopy, IR spectroscopy, high resolution mass spectrometry (ESI-MS), absorption spectroscopy and fluorescence spectroscopy. We first consider the ^{1}H NMR data. In general, a bacteriochlorin that has C_{2h} symmetry (such as the **H-BC**-type macrocycles lacking the fifth ring or the 15-bromo substituent) exhibits a relatively simple ^{1}H NMR spectrum. Introduction of a single substituent (*e.g.*, 5-methoxy, 15-bromo or ring E) results in C_s symmetry whereupon a number of otherwise identical structural elements in the respective A,C and B,D rings become magnetically non-equivalent and split into distinct signals. The non-equivalent entities include the two pyrrolic N–H protons, the pair of geminal dimethyl groups, the CH_2 group in each of the two pyrroline rings, and any β-pyrrolic substituents (*e.g.*, methyl unit of the acetyl group in **MeOBC-MeA**). The synthetic bacteriochlorins synthesized to date typically exhibit a broad upfield peak in the region δ −2.40–0.12 ppm (pyrrolic N–H protons), a singlet between δ 1.81–2.02 ppm (geminal dimethyl groups), and a singlet between δ 4.30–4.50 ppm (pyrroline CH_2 groups). The ^{1}H NMR signal for the 5-methoxy group generally resonates in the region δ 3.68–4.48 ppm.[44–46]

The ^{1}H NMR spectrum of bacterio-13^1-oxophorbine **MeOBOP** displays the aforementioned features characteristic of bacteriochlorins with C_s symmetry. In addition, the two protons at the 13^2-position (ring E) resonate as a singlet at δ 4.88 ppm, to be compared with the ABX pattern of the diastereotopic 13^2-protons of bacteriopyro-13^1-oxophorbines (owing to the presence of stereocenters at positions 17 and 18 in the neighboring ring).[3,29,36,60] The chemical shift range is comparable to those of bacteriochlorophyll *a* derivatives

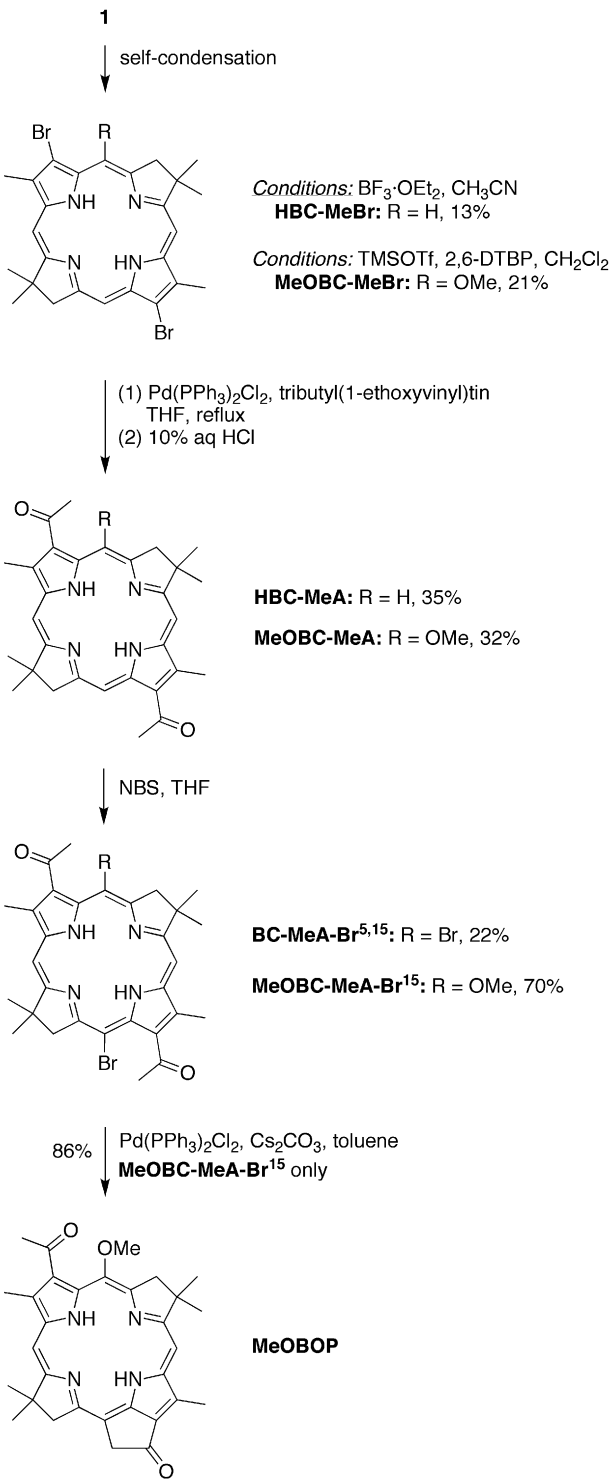

Scheme 5 Synthesis of a bacterio-13^1-oxophorbine.

(δ 4.76–5.31 ppm) and synthetic chlorophyll analogues (13^1-oxophorbines, δ 5.03–5.16 ppm).[53,59]

The bacteriochlorin-13,15-dicarboximides **MeOBC-I** and **HBC-I** also display ^{1}H NMR spectral features characteristic of bacteriochlorins with C_s symmetry. The ^{1}H NMR spectra of **MeOBC-I** and **HBC-I** also provide information on the formation of the imide and/or isoimide ring, which are ever-present possibilities in the imidation process. In chlorin

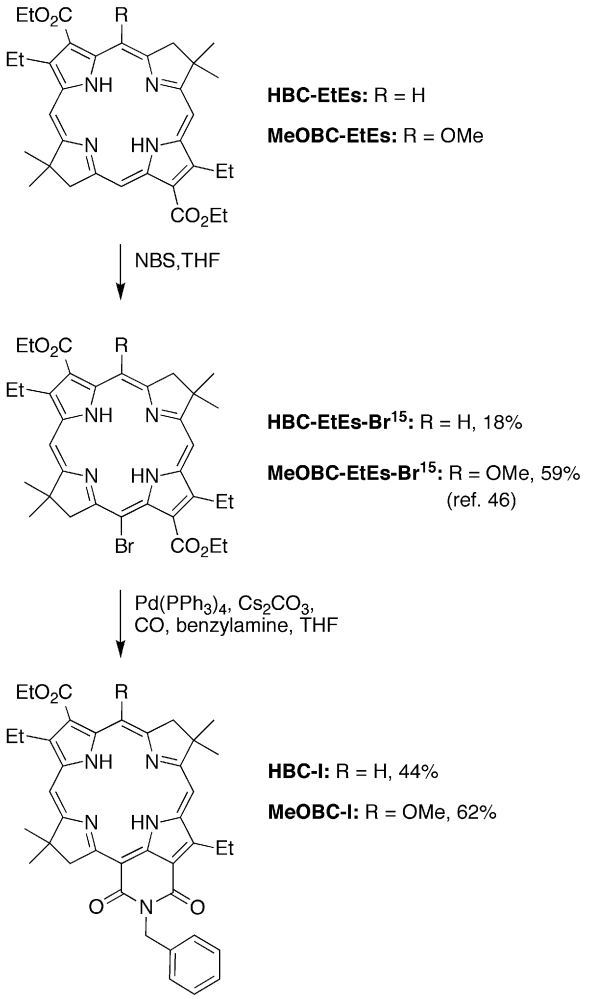

Scheme 6 Synthesis of a bacteriochlorin-13,15-dicarboximide.

chemistry, the 13-ester-15-bromochlorin gave exclusively the chlorine-imide, whereas imide and isoimide mixtures were sometimes observed upon reaction of the 13-carbamoyl-15-bromochlorin.[54] A convenient method for distinguishing the two isomers relied on the chemical shift of the methylene protons of the *N*-benzyl (iso)imide: δ 5.6 ppm for the chlorin-imides *versus* 5.2 ppm for the corresponding chlorin-isoimides.[54] In the work reported herein, **MeOBC-I** and **HBC-I** were each obtained from the corresponding 13-ester-15-bromobacteriochlorin, and the benzylic protons of **MeOBC-I** and **HBC-I** resonated at δ 5.67 and 5.68 ppm, respectively. Such data by analogy with the chlorins are consistent with the formation of bacteriochlorin-imides.

The IR spectrum of **MeOBOP** shows carbonyl stretching bands at 1687 and 1630 cm^{-1}, along with bands at 2918–2954 cm^{-1} (C–H) and 3435 cm^{-1} (N–H). In comparison, the carbonyl stretch of a bacteriochlorin in a dyad (bacterio-pyropheophorbide–pyromellitimide) occurs at 1695 cm^{-1},[3] whereas that of a zinc chelate of a bacterio-13^1-oxophorbine appears at 1682 cm^{-1}.[61] The carbonyl stretch for a variety of methyl pyropheophorbides (chlorins) occurs in the region 1650–1699 cm^{-1}.[62,63] Kunieda and Tamiaki have used IR extensively to identify hydrogen-bonding with hydroporphyrin carbonyl groups in supramolecular assemblies.[61,63] The IR

spectra of **MeOBC-I** and **HBC-I** show carbonyl stretching bands in the range of 1647–1682 cm^{-1}, along with bands in the region 2848–2959 cm^{-1} (C–H) and 3386–3435 cm^{-1} (N–H). To our knowledge, IR data have not been reported for other bacteriochlorin-imides.

V Absorption spectra

The annulated bacteriochlorins prepared herein exhibit characteristic bacteriochlorin absorption spectra,[1] with near-ultraviolet (Soret or B) bands, a long-wavelength feature, the $Q_y(0,0)$ band, in the near-infrared region of comparable peak intensity, and the weaker Q_x bands in the intervening region (500–600 nm). The position of the long wavelength absorption band of a photochemically active species is of central importance, defining not only the spectral region where absorption occurs but also the energy of the lowest singlet excited-state, which dominates key photophysical properties. These properties include fluorescence and, for the native bacteriochlorophylls, the energy- and electron-transfer reactions of photosynthesis.

Prior studies with synthetic bacteriochlorins have shown that the position of the $Q_y(0,0)$ band could be tuned from 707 nm to 792 nm (typically measured in toluene).[51,44–46] The synthetic bacterio-13^1-oxophorbine **MeOBOP** (733 nm) absorbs in this range, to be compared with that of methyl bacteriopyropheophorbide *a* (754 nm in CH_2Cl_2).[29] Bacteriopheophytin *a* (**BPh-a**), which differs from methyl bacteriopyropheophorbide *a* owing to the presence of a 13^2-methoxycarbonyl group and a long alkyl ester chain, also absorbs at 750–760 nm in hydrocarbon solvents.[64,65] The bacteriochlorin-imides **MeOBC-I** (793 nm) and **HBC-I** (818 nm) exhibit $Q_y(0,0)$ bands that extend further into the near infrared. The $Q_y(0,0)$ band of bacteriochlorin-imides derived from bacteriochlorophyll *a* occurs in the same spectral range (800–830 nm).[32,33,36]

The spectra of **MeOBOP**, **MeOBC-I** and **HBC-I** in toluene are shown in Fig. 1. The $Q_y(0,0)$ positions are listed in Table 1 along with those of a number of bacteriochlorin benchmarks that lack the annulated ring E. Reference molecules for **MeOBOP** include a set of 3,13-diacetylbacteriochlorins: **MeOBC-MeA** (743 nm), **MeOBC-A** (740 nm), **HBC-MeA** (766 nm) and **HBC-A** (768 nm). The first three of these 3,13-diacetylbacteriochlorins were prepared here (Schemes 2 and 5) whereas **HBC-A** (Chart 2) was synthesized previously.[45] Comparison among the four 3,13-diacetylbacteriochlorins shows that (1) the 5-methoxy group results in an average 25 nm hypsochromic shift in the $Q_y(0,0)$ position, and (2) the 2,12-dimethyl groups have little ($\leqslant$3 nm) effect on the $Q_y(0,0)$ position. The first point, regarding the 5-methoxy group, is also made upon comparison of the $Q_y(0,0)$ positions of bacteriochlorins **MeOBC-EtEs** (739 nm) and **HBC-EtEs** (761 nm).[46] The latter two compounds (Scheme 6) serve as benchmarks for the two bacteriochlorin-imides (**MeOBC-I** and **HBC-I**): the benchmarks contain the 2,12-diethyl and 3-ester groups but lack the 13,15-dicarboximide moiety. The $Q_y(0,0)$ position for **MeOBC-I** (793 nm) and **HBC-I** (818 nm), like the three pairs of bacteriochlorins noted above, shows a 25 nm hypsochromic shift due to the 5-methoxy group. Interestingly, the impact of the 5-methoxy group is diminished in bacteriochlorins that lack a carbonyl moiety (acetyl, ester, imide) at the 3,13-positions. This point is seen upon comparison of the $Q_y(0,0)$ positions of bacteriochlorins **MeOBC** (709 nm)[46] and **HBC** (713 nm)[45] that bear one or no substituents, respectively, other than the geminal dimethyl groups (Chart 2).

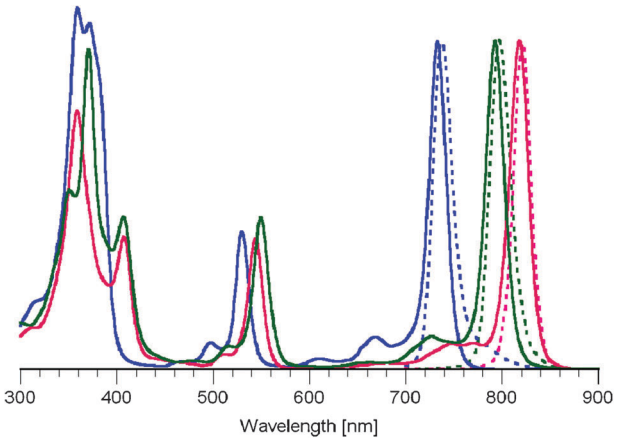

Fig. 1 Absorption (— solid lines) and emission (- - - dashed lines) spectra (normalized) in toluene at room temperature of **MeOBOP** (blue), **MeOBC-I** (green), and **HBC-I** (magenta).

VI Fluorescence spectra, quantum yields, and singlet excited-state lifetimes

The fluorescence spectra of **MeOBOP**, **MeOBC-I** and **HBC-I** in toluene are shown in Fig. 1 (dotted lines). Each fluorescence spectrum is dominated by the $Q_y(0,0)$ band, which lies $\sim$5 nm to longer wavelength than the corresponding $Q_y(0,0)$ absorption feature. The same is generally true for the benchmark bacteriochlorins listed in Table 1; exceptions include **HBC-EtEs** and **MeOBC-EtEs**, which show larger (10–15 nm) Stokes shifts, suggesting greater changes in structure or solvent interactions upon photoexcitation.

The bathochromic shift of the $Q_y(0,0)$ band of **MeOBOP**, **MeOBC-I** and **HBC-I** (733 nm, 793 nm, 818 nm) is accompanied by a decrease in the fluorescence yield (0.19, 0.052, 0.036) and shortening of the singlet excited-state lifetime (4.6 ns, 2.2 ns, 1.9 ns). The same is true of the benchmark bacteriochlorins. These data are plotted in Fig. 2C and D and listed in Table 1. For comparison, the singlet excited-state lifetime of bacteriopheophytin *a* is 2.0–2.7 ns and has a $Q_y(0,0)$ band at 750–760 nm in organic solvents (Table 1).[64,65] Thus, the two synthetic bacteriochlorin-imides absorb at significantly longer wavelengths (by $\sim$40 and $\sim$70 nm) than the natural pigment and yet have comparable excited-state lifetime.

VII Frontier molecular orbitals and electronic properties

The energies and electron-density distributions of the frontier molecular orbitals (MOs) of the bacterio-13^1-oxophorbine, bacteriochlorin-imides, and benchmark compounds were obtained from density functional theory (DFT) calculations. Such methods were also applied to the fictive bacteriochlorin **MeOBC-MeAMe**[15] (Chart 3), which differs from the benchmark compound **MeOBC-MeA** in the addition of a 15-methyl substituent. Examination of **MeOBC-MeAMe**[15] provides

Table 1 Photophysical properties of bacteriochlorin compounds[a]

Compound	Cmpd code for Fig. 2	λ_{Q_y} abs/nm	λ_{Q_y} em/nm	I_{Q_y}/I_B[b]	Φ_f[c]	τ_s[d]/ns	HOMO − LUMO[e]/eV	HOMO-1 − LUMO + 1[f]/eV
Targets:								
HBC-I	*a*	818	823	1.3	0.036	1.9	1.92	4.01
MeOBC-I	*b*	793	798	1.0	0.052	2.2	2.02	3.92
MeOBOP	*h*	733	739	0.93	0.19	4.6	2.18	3.86
Benchmarks:								
HBC	*i*	713	716	0.85	0.17	4.0	2.26	4.06
HBC-A	*c*	768	771	1.2	0.11	2.9	2.05	3.95
HBC-MeA		766					2.02	3.94
HBC-EtEs	*d*	761	775	0.94	0.14	3.3	2.10	3.98
MeOBC	*j*	709	711	0.87	0.25	5.0	2.28	3.98
MeOBC-A	*f*	740	747	0.96	0.14	3.8	2.14	3.88
MeOBC-MeA	*e*	743	749	0.95	0.13	3.4	2.14	3.87
MeOBC-EtEs	*g*	739	749	1.1	0.17	4.3	2.16	3.91
BPh-a[g]		758	768	0.69	0.10	2.7	2.03[h]	3.89[h]
Fictive:								
MeOBC-MeAMe[15]							2.17	3.80

[a] In toluene at room temperature unless noted otherwise. [b] Ratio of the peak intensities of the $Q_y(0,0)$ and B bands. [c] Fluorescence quantum yield (error ± 7%). [d] Lifetime of the lowest singlet excited state measured using fluorescence techniques (error ± 7%). Values for several of the benchmark compounds were reported in ref. 45. [e] Energy gap between the LUMO and HOMO orbitals. [f] Energy gap between the LUMO + 1 and HOMO-1 orbitals. [g] Values in toluene. The values in ethanol are λ_{abs} = 750 nm, λ_{em} = 768 nm, I_{Q_y}/I_B = 0.39, Φ_f = 0.081, and τ_s = 2.3 ns. A value of τ_s = 2.0 ns in acetone/methanol 7 : 3 was found in ref. 65. [h] DFT calculations were performed with the truncated phytyl tail $-CH_2CH{=}C(CH_3)(CH_2CH_3)$.

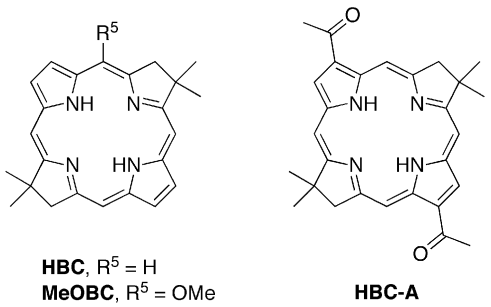

Chart 2 Benchmark bacteriochlorins prepared previously.[45]

deeper insight into the origin of the effects caused by the formation of the fifth ring. The four frontier molecular orbitals and energy levels for nine compounds are shown in Table 2.

The key results of the DFT calculations for **MeOBOP**, **MeOBC-I**, **HBC-I** and representative benchmark synthetic and fictive compounds are summarized in Fig. 2. This figure shows the characteristics of the four frontier orbitals: the highest occupied molecular orbital (HOMO), the lowest unoccupied molecular orbital (LUMO), the HOMO-1, and LUMO + 1. The energies of these MOs are plotted as a function of the $Q_y(0,0)$ absorption-band energy/wavelength in Fig. 2A, and analogous plots for the HOMO − LUMO energy gap and HOMO-1 − LUMO + 1 energy gap are shown in Fig. 2B. In each of these plots, the data for the key target compounds (**MeOBOP**, **MeOBC-I** and **HBC-I**) are given by closed symbols and those for the benchmark bacteriochlorins by open symbols. The values for the HOMO − LUMO and HOMO-1 − LUMO + 1 energy gaps for the various compounds are listed in Table 1. These two energy gaps are relevant to the spectral analysis given below.

The salient points from the DFT calculations and the relationship to the observed spectral properties are as follows:

(1) The slopes of the trend lines given in Fig. 2A show that the LUMO (m = 3.2) is more strongly connected with the wavelength/energy of the $Q_y(0,0)$ absorption band than are the HOMO (m = 1.8), LUMO + 1 (m = 2.3) and HOMO-1 (m = 2.4). These differences can be traced to the generally greater electron density in the LUMO at the substituent sites (Table 2). The most important sites in this regard are the 3,13-positions of the carbonyl substituents (acetyl, ester, imide) of **MeOBOP**, **MeOBC-I**, **HBC-I** and the benchmark bacteriochlorins. These sites (and the 2,12-positions) are on the molecular y-axis, which is the axis on which the Q_y optical transition is polarized.

(2) In Gouterman's four-orbital model,[66,67] the position of the $Q_y(0,0)$ absorption band depends on the average value of the HOMO − LUMO energy gap and the HOMO-1 − LUMO + 1 energy gap. Because of the trends in the individual molecular orbitals described above and shown in Fig. 2A, there is a much greater variation in the HOMO − LUMO energy gap *versus* the HOMO-1 − LUMO + 1 energy gap for **MeOBOP**, **MeOBC-I**, **HBC-I** and the benchmark bacteriochlorins (Table 1). The consequence is a much greater magnitude of the slope of the trend line for the HOMO − LUMO energy gap (m = 1.4) *versus* the HOMO-1 − LUMO + 1 energy gap (m = −0.05) plotted against the $Q_y(0,0)$ wavelength/energy (Fig. 2B). Consequently, the wavelength/position of the $Q_y(0,0)$ band is dominated by the HOMO − LUMO energy gap for the bacterio-13^1-oxophorbine, bacteriochlorin-imides, and bacteriochlorins described here. In turn, following the findings given in point (1), the spectral position is dictated much more strongly by the dependence of the LUMO than the HOMO on the macrocycle-substituent pattern for these molecules.

(3) The DFT calculations reproduce the effect of the 5-methoxy group on the position of the $Q_y(0,0)$ wavelength/energy. This can be seen by comparing the value for the $Q_y(0,0)$ wavelength and the HOMO − LUMO energy gap for the following pairs of 3,13-dicarbonyl-containing (acetyl, ester, imide) compounds (Table 1): **MeOBC-I**

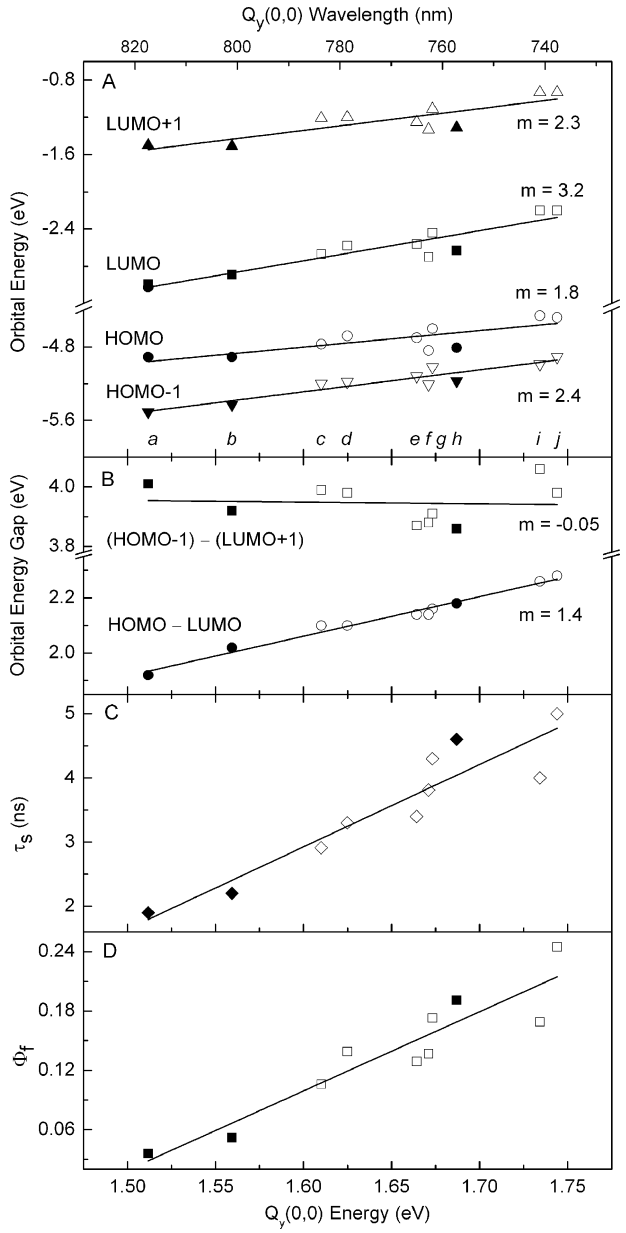

Fig. 2 Orbital energies, energy gaps, singlet excited-state lifetime, and fluorescence yield as a function of the $Q_y(0,0)$ energy (bottom axis) and wavelength (top axis). For each plot, the solid symbols are for the three target compounds, **MeOBOP**, **MeOBC-I** and **HBC-I**, and the open symbols are for the benchmark bacteriochlorins. The letter code (*a–j*) at the bottom of panel A gives the left-to-right order of the data points for each plot in the figure and identifies the compounds as listed in the first two columns of Table 1.

(793 nm, 2.02 eV) *versus* **HBC-I** (818 nm, 1.92 eV); **MeOBC-EtEs** (739 nm, 2.16 eV) *versus* **HBC-EtEs** (761 nm, 2.10 eV); **MeOBC-MeA** (743 nm, 2.14 eV) *versus* **HBC-MeA** (766 nm, 2.02 eV); and **MeOBC-A** (740 nm, 2.14 eV) *versus* **HBC-A** (768 nm, 2.05 eV). For these pairs of compounds (with *versus* without the 5-methoxy group), the average bathochromic shift is 24 nm and the average shift in the HOMO – LUMO gap to lower energy is 0.09 eV. By comparison, the values for **MeOBC** (709 nm, 2.28 eV) *versus* **HBC** (713 nm, 2.26 eV)

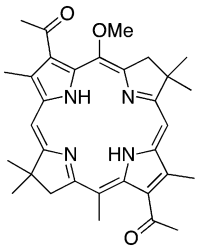

MeOBC-MeAMe[15]

Chart 3 Fictive bacteriochlorin for which DFT calculations were performed.

reveal a much smaller spectral shift of 4 nm and a corresponding smaller molecular-orbital energy-gap shift of 0.02 eV. Obviously there is interplay between the electron-donating ability of the 5-methoxy group and the sensitivity of the 3,13-positions to the presence of auxochromes such as carbonyl moieties.

(4) The DFT calculations of the benchmark compounds reproduce the finding that the 2,12-dimethyl groups of bacterio-13[1]-oxophorbine **MeOBOP**, and in analogy the 2-ethyl group of **MeOBC-I** and **HBC-I**, have little effect. This result is shown by the $Q_y(0,0)$ wavelength and the HOMO – LUMO energy gap for the following pairs of compounds: **HBC-A** (768 nm, 2.05 eV) *versus* **HBC-MeA** (766 nm, 2.02 eV); and **MeOBC-A** (740 nm, 2.14 eV) *versus* **MeOBC-MeA** (743 nm, 2.14 eV). In both cases the presence of the 2,12-dimethyl groups results in $\leq$3 nm spectral shift and a $\leq$0.03 eV shift in the molecular-orbital energy gap. Collectively, these results suggest that the alkyl groups at the 2- or 12-positions of **MeOBOP**, **MeOBC-I** and **HBC-I**, and by implication the native photosynthetic pigments, such as **BPh-a** (Table 2), play an insignificant role in determining the spectral properties of these molecules.

(5) The data and analysis given above (Table 1 and Fig. 1 and 2) provide insights into which substituents are most responsible for the spectral characteristics of **MeOBOP** *versus* that of the benchmark bacteriochlorin **MeOBC**. The $Q_y(0,0)$ position and HOMO – LUMO gap for **MeOBC** (709 nm, 2.28 eV) are strongly affected upon the addition of the 3,13-diacetyl groups (**MeOBC-A**: 740 nm, 2.14 eV), with little further effect upon addition of the 2,12-dimethyl groups (**MeOBC-MeA**: 743 nm, 2.14 eV). The final step to obtain **MeOBOP** (733 nm, 2.18 eV) is closure to form the five-membered ring. The latter can be thought of as first, placement of a substituent at the 15-methyl group, and second, ring closure accompanied by structural/electronic effects such as ring strain and shift toward planarity. To gain insights into the effect of the 15-substituent, DFT calculations were carried out on the fictive bacteriochlorin **MeOBC-MeAMe**[15], wherein a methyl group is placed at the 15-position (Chart 3, Tables 1 and 2). The HOMO – LUMO energy gap (2.17 eV) for this fictive compound is between those for **MeOBC-MeA** (2.14 eV) and **MeOBOP** (2.18 eV), consistent with a modest effect of substitution at the 15-position. Given the small (0.03–0.04 eV) energy shifts involved, however, the effects of 15-substitution *versus* ring closure (once the 13-acetyl group is in place) are of uncertain relative magnitude in dictating the ultimate spectral properties of the bacterio-13[1]-oxophorbine chromophores.

Table 2 Molecular-orbital energies and electron-density distributions of bacteriochlorin compounds

	HBC-I	MeOBC-I	MeOBOP	BPh-a[a]	MeOBC-MeAMe[15]	MeOBC-MeA	MeOBC-A	MeOBC	HBC
Structure	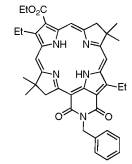	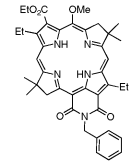	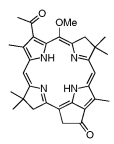	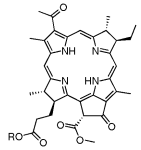	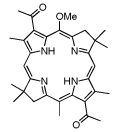	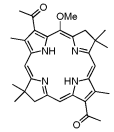	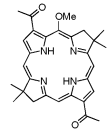	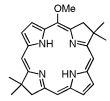	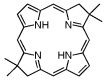
LUMO + 1/eV	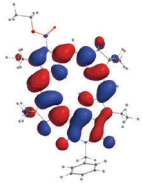	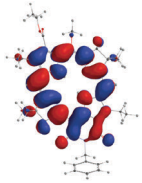	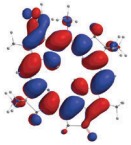	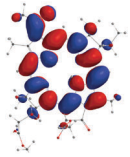	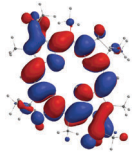	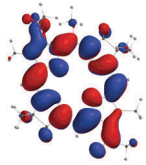	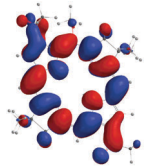	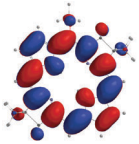	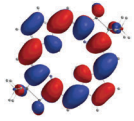
	−1.50	−1.51	−1.31	−1.41	−1.22	−1.25	−1.33	−0.93	−0.93
LUMO/eV	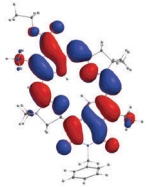	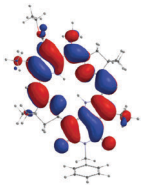	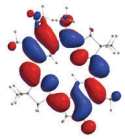	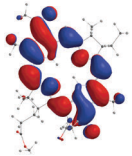	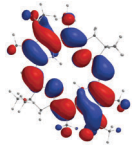	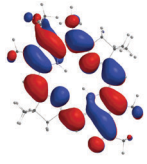	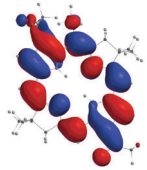	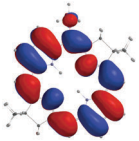	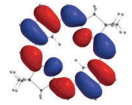
	−2.99	−2.89	−2.63	−2.84	−2.50	−2.56	−2.70	−2.20	−2.20
HOMO/eV	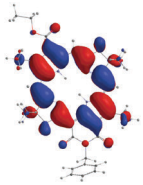	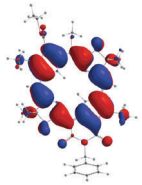	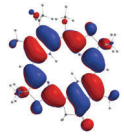	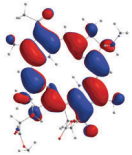	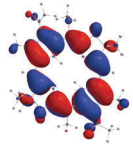	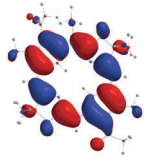	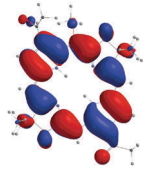	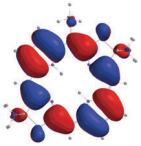	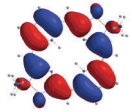
	−4.91	−4.91	−4.81	−4.87	−4.67	−4.70	−4.84	−4.48	−4.46
HOMO-1/eV	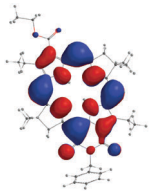	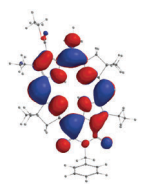	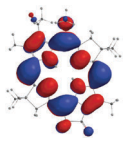	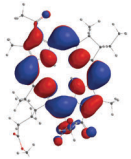					
	−5.51	−5.43	−5.17	−5.30	−5.02	−5.12	−5.21	−4.91	−4.99

[a] For **BPh-a**, calculations were performed with a truncated phytyl tail [–CH_2–CH=$C(CH_3)(CH_2CH_3)$], which is omitted in the display here.

Outlook

Bacteriochlorophylls are Nature's pigments for absorption of sunlight in the near-infrared region. The ability to utilize such compounds in diverse artificial systems—such as artificial photosynthesis, clinical diagnostics, and photomedicine—depends on versatile synthetic methods that afford stable macrocycles and that enable the spectral properties to be tuned at will. The designs we have chosen employ a geminal dimethyl group in each pyrroline ring to ensure stability toward adventitious dehydrogenation. The resulting synthetic bacteriochlorins thus differ slightly in structure from the natural pigments, yet are more robust toward routine handling and synthetic manipulation. Here we have explored the ability to install an exocyclic ring, either the five-membered isocyclic ring as occurs in all bacteriochlorophylls, or the six-membered imide ring characteristic of derivatives of bacteriochlorophylls commonly known as bacteriopurpurinimides.

Of the *de novo* synthesized bacteriochlorins that we have prepared to date, **MeOBC**[46] and **HBC**[45] are at the shorter wavelength end of the range of $Q_y(0,0)$ absorption positions while the two bacteriochlorin-imides **MeOBC-I** and **HBC-I** are at the longer extreme. A naturally occurring bacteriochlorin (wherein each pyrroline ring bears a geminal dialkyl unit and an oxo group) known as tolyporphin A absorbs at 678 nm.[68] The ability to tune the absorption band almost at will from ~680–820 nm bodes well for the use of synthetic bacteriochlorins, bacterio-13^1-oxophorbines, and bacteriochlorin-13,15-dicarboximides in diverse photochemical applications. The pursuit of such applications will be facilitated by the fluorescence yields (0.036–0.19), singlet excited-state lifetimes (1.9–4.6 ns), and photostability of the bacterio-13^1-oxophorbine and bacteriochlorin-13,15-dicarboximides prepared herein, as well as the obvious sites for synthetic elaboration provided by the keto and *N*-imide groups of the annulated ring E.

Experimental section

I General methods

^{1}H NMR spectra (300 MHz) and ^{13}C NMR spectra (100 MHz) were collected at room temperature in $CDCl_3$. Silica gel (40 μm average particle size) was used for column chromatography. All solvents were reagent grade and were used as received unless noted otherwise. THF was freshly distilled from sodium/benzophenone ketyl. Laser-desorption mass spectrometry was performed without any matrix. Electrospray ionization mass spectrometry (ESI-MS) data are reported for the molecule ion or protonated molecule ion. Known compounds 3-methyl-pyrrole-2-carboxaldehyde (**2**),[57] 1,1-dimethoxy-4-methyl-3-penten-2-one (**5**),[44] and two bacteriochlorins (**HBC-EtEs**, **MeOBC-EtEs-Br**[15])[46] were prepared according to literature procedures.

3,13-Diacetyl-5-methoxy-8,8,18,18-tetramethylbacteriochlorin (MeOBC-A). Following a procedure for replacement of a bromo group with an acetyl group on a bacteriochlorin with modification,[46,58] a mixture of **MeOBC-Br** (108 mg, 0.194 mmol), tributyl(1-ethoxyvinyl)tin (135 μL, 0.388 mmol), and $(PPh_3)_2PdCl_2$ (56 mg, 0.078 mmol) was heated in acetonitrile/DMF [20 mL (3 : 2)] at 85 °C for 1.5 h. The reaction mixture was treated with 10% aqueous HCl (50 mL) at room temperature for 20 min and then diluted with CH_2Cl_2. The reaction mixture was poured into a saturated aqueous solution of $NaHCO_3$ and extracted with dichloromethane. The organic layer was dried (Na_2SO_4), concentrated and chromatographed (silica, CH_2Cl_2) to afford a purple solid (64 mg, 68%): ^{1}H NMR δ −1.68 (br s, 1H), −1.31 (br s, 1H), 1.90 (s, 6H), 1.95 (s, 6H), 3.08 (s, 3H), 3.16 (s, 3H), 4.18 (s, 3H), 4.36 (s, 2H), 4.39 (s, 2H), 8.54 (s, 1H), 8.63 (s, 1H), 8.66 (d, J = 2.2 Hz, 1H), 9.08 (d, J = 1.93 Hz, 1H), 9.77 (s, 1H); ^{13}C NMR δ 29.9, 31.0, 31.3, 33.2, 45.5, 46.1, 48.2, 51.6, 64.9, 97.6, 99.6, 99.8, 121.3, 125.7, 128.3, 129.1, 133.0, 135.1, 135.6, 135.7, 135.9, 157.2, 162.5, 169.2, 172.8, 197.0, 202.5; ESI-MS obsd 485.25401; calcd 485.25527 [$(M + H)^+$, M = $C_{29}H_{32}N_4O_3$]; λ_{abs} (CH_2Cl_2) 362, 530, 742 nm.

3,13-Bis(2-methyl-1,3-dioxolan-2-yl)-5-methoxy-8,8,18,18-tetramethylbacteriochlorin (MeOBC-K). Following a known procedure,[56] a solution of **MeOBC-A** (20.0 mg, 0.0413 mmol) in CH_2Cl_2 (3.5 mL) was treated with ethylene glycol (470 μL, 82.6 mmol) and TMSCl (422 μL, 3.30 mmol). The mixture was stirred at room temperature for 6 h. A saturated aqueous solution of $NaHCO_3$ was added and the mixture was extracted with CH_2Cl_2. The organic layer was separated, dried (Na_2SO_4) and concentrated under vacuum. Column chromatography (alumina, CH_2Cl_2) afforded a green solid (17 mg, 72%): ^{1}H NMR δ −2.06 (br s, 1H), −1.86 (br s, 1H), 1.945 (s, 6H), 1.951 (s, 6H), 2.33 (s, 3H), 2.40 (s, 3H), 4.12–4.33 (m, 4H), 4.25 (s, 3H), 4.34–4.50 (m, 4H), 4.42 (s, 2H), 4.44 (s, 2H), 8.576 (s, 1H), 8.584 (s, 1H), 8.73 (d, J = 2.75 Hz, 1H), 8.79 (d, J = 2.75 Hz, 1H), 9.08 (s, 1H); LD-MS obsd 572.7, calcd 572.3 ($C_{33}H_{40}N_4O_5$); λ_{abs} (CH_2Cl_2) 356, 367, 505, 715 nm.

8-Bromo-2,3-dihydro-1-(1,1-dimethoxymethyl)-3,3,7-trimethyldipyrrin (1). Following a procedure for the synthesis of bromodihydrodipyrrin-acetals,[50] in a first flask a solution of **6-H** (4.77 g, 12.2 mmol) in freshly distilled THF (30 mL) at 0 °C was treated with freshly prepared NaOMe (3.3 g, 61 mmol). The resulting mixture was stirred and degassed by bubbling argon through the solution for 45 min. In a second flask purged with argon, $TiCl_3$ (46 mL, 20% in 3% HCl solution, 73 mmol), THF (90 mL), NH_4OAc (35 g, 0.46 mol), and degassed water (50 mL) were combined under argon and the solution was degassed by bubbling argon through the solution for 45 min. Then the first flask mixture was transferred *via* cannula to the buffered $TiCl_3$ solution. The resulting mixture was stirred at room temperature for 16 h under argon. A saturated solution of aqueous $NaHCO_3$ (300 mL) was added followed by ethyl acetate (200 mL). The mixture was extracted with ethyl acetate. The organic layer was dried (Na_2SO_4), concentrated to a brown oil, dried under high vacuum for 2 h, and chromatographed on a short alumina column (neutral alumina, CH_2Cl_2) to give a light brown oil (1.40 g, 34%): ^{1}H NMR δ 1.22 (s, 6H), 2.10 (s, 3H), 2.62 (s, 2H), 3.44 (s, 6H), 5.01 (s, 1H), 5.80 (s, 1H), 6.73–6.84 (m, 1H), 10.66 (br s, 1H); ^{13}C NMR δ 10.1, 29.4, 40.5, 48.4, 54.8, 99.6, 102.9, 105.1, 117.3, 117.9, 127.5, 159.9, 174.7; ESI-MS obsd 341.0865, calcd 341.0859 [$(M + H)^+$, M = $C_{15}H_{21}BrN_2O_2$].

4-Bromo-3-methylpyrrole-2-carboxaldehyde (3). Following a general procedure,[50] a stirred solution of 3-methyl-pyrrole-2-carboxaldehyde (**2**, 5.63 g, 51.6 mmol) in THF (52 mL) was cooled to 0 °C. NBS (9.19 g, 51.6 mmol; reagent grade, unrecrystallized) was added all at once. The reaction mixture was stirred for 15 min at 0 °C under argon before the solvent was removed on a rotary evaporator. The resulting solid was dried under high vacuum for 2 h. Water (100 mL, room temperature) was added to the flask and the suspension was filtered (Büchner funnel). The filter cake was washed with an additional 100 mL of water. The solid filtered material was recrystallized from water/ethanol as follows. The solid filtered material was transferred to a 250 mL round bottom flask equipped with a reflux condenser. Water/ethanol (150 mL, 5 : 1) was added and the mixture was refluxed in a hot water bath until all solid material had dissolved. Upon allowing the solution to cool to room temperature the product crystallized. The mixture was cooled to 4 °C for 2 h to promote more crystallization. The mixture was vacuum-filtered and the resulting off-white crystals were dried under high vacuum for 24 h (7.78 g, 80%): mp 140–143 °C; ^{1}H NMR δ 2.32 (s, 3H), 7.08 (d, J = 3.3 Hz, 1H), 9.60 (s, 1H), 9.95 (br s, 1H); ^{13}C NMR δ 9.8, 101.7, 126.0, 129.3, 131.7, 177.9; ESI-MS obsd 187.9708, calcd 187.9706 [$(M + H)^+$, M = C_6H_6BrNO].

4-Bromo-3-methyl-2-formyl-*N*-tosylpyrrole (3-Ts). Following a general procedure,[50] a stirred suspension of 60% NaH (2.5 g, 62 mmol) in dry THF (42 mL, distilled) was cooled to 0 °C under argon. The mixture was treated portionwise with **3** (7.78 g, 41.4 mmol). The mixture was stirred for 30 min at 0 °C before treating all at once with *p*-toluenesulfonyl chloride (8.00 g, 41.4 mmol). The reaction mixture was stirred at room temperature for 3 h, whereupon water (100 mL) was slowly added to quench the reaction. Ethyl acetate (100 mL) was added, and the organic layer was separated. The organic layer was washed with brine, dried (Na_2SO_4), and concentrated to a solid. The solid was dried under high vacuum for 2 h. The crude solid material was dissolved in 100 mL hexanes/ethyl acetate (5 : 1) by refluxing in a hot water bath. Upon allowing the solution to cool to room temperature the product crystallized. The mixture was cooled overnight at −10 °C to promote additional crystallization. The mixture was vacuum-filtered, and the resulting light brown crystals were dried under high vacuum (9.73 g, 69%): mp 152–155 °C; ^{1}H NMR δ 2.29 (s, 3H), 2.43 (s, 3H), 7.34 (d, J = 8.5 Hz, 2H), 7.55 (s, 1H), 7.76 (d, J = 8.5 Hz, 2H), 10.14 (s, 1H); ^{13}C NMR δ 2.1, 22.0, 106.2, 126.8, 127.6, 129.1, 130.6, 135.2, 136.4, 146.5, 180.1; anal. calcd for $C_{13}H_{12}BrNO_3S$: C, 45.63; H, 3.53; N, 4.09%. found: C, 45.71; H, 3.44; N, 4.11%.

4-Bromo-3-methyl-2-(2-nitroethyl)-*N*-tosylpyrrole (4-Ts). Following a general procedure,[50] a stirred mixture of **3-Ts** (7.73 g, 28.5 mmol) in the form of a finely ground powder, potassium acetate (2.24 g, 22.8 mmol), methylamine hydrochloride (1.54 g, 22.8 mmol), and acetic acid (0.1 mL) in absolute ethanol (10 mL) was treated with nitromethane (4.0 mL, 78 mmol). The mixture was stirred for 2 h, whereupon water was added (100 mL) and the resulting yellow precipitate was filtered by vacuum filtration. The solid filtered material was washed with water (200 mL) followed by cold ethanol (~100 mL, 0 °C) until the eluant was clear. The yellow filtered solid was dried overnight under high vacuum. The crude solid material was dissolved in dry THF (117 mL, distilled). The solution was cooled to −10 °C (internal temperature, using an acetone bath with a few pieces of dry ice) under argon. The solution was treated with 95% $LiBH_4$ (0.64 g, 28 mmol) all at once under vigorous stirring. The reaction mixture was stirred for ~15 min at −10 °C, until all of the starting material disappeared (starting material: $CH{=}CHNO_2$: d, J = 13.6 Hz, 8.56 ppm; product: $CH_2CH_2NO_2$: t, J = 7.3 Hz, 4.54 ppm and 3.36 ppm), whereupon the reaction mixture was quenched by slowly adding a cold saturated aqueous NH_4Cl solution (200 mL, 0 °C). The mixture was extracted with ethyl acetate (200 mL). The organic layer was washed with brine, dried (Na_2SO_4), and concentrated to a solid. The solid was dried under high vacuum for 2 h. The crude solid material was dissolved in 100 mL of 2-propanol by refluxing in a hot water bath. Upon cooling the solution to −10 °C the product crystallized. The mixture was vacuum-filtered, and the resulting light brown crystals were dried under high vacuum (9.03 g, 82%): mp 85 °C; ^{1}H NMR δ 1.92 (s, 3H), 2.43 (s, 3H), 3.36 (t, J = 7.3 Hz, 2H), 4.54 (t, J = 7.3 Hz, 2H), 7.34 (d, J = 8.4 Hz, 2H), 7.34 (s, 1H), 7.66 (d, J = 8.4 Hz, 2H); ^{13}C NMR δ 10.5, 21.9, 24.3, 74.3, 105.2, 121.7, 124.3, 124.9, 126.9, 130.6, 135.6, 146.0; ESI-MS obsd 387.0024, calcd 387.0009 [$(M + H)^+$, M = $C_{14}H_{15}BrN_2O_4S$].

6-(4-Bromo-3-methyl-*N*-tosylpyrrol-2-yl)-1,1-dimethoxy-4,4-dimethyl-5-nitrohexan-2-one (6-Ts). Following a general procedure,[50] a mixture of **4-Ts** (9.00 g, 23.3 mmol) and 1,1-dimethoxy-4-methyl-3-penten-2-one (11.1 g, 69.9 mmol, 3 equiv) was treated with DBU (10.5 mL, 69.9 mmol). The reaction mixture was stirred for 15 min under argon. A saturated solution of cold aqueous NH_4Cl (50 mL, 0 °C) was added. The mixture was extracted with ethyl acetate (100 mL). The organic layer was washed with brine, dried (Na_2SO_4), concentrated and dried overnight under high vacuum. Addition of diethyl ether (50 mL) to the resulting solid, trituration, and filtration afforded a pale brown solid (11.0 g, 86%): mp 114–115 °C; ^{1}H NMR δ 1.22 (s, 3H), 1.27 (s, 3H), 1.85 (s, 3H), 2.42 (s, 3H), 2.64, 2.74 (AB, ^2J = 19.0 Hz, 2H), 3.15 (ABX, $^2J_{AB}$ = 15.4 Hz, $^3J_{BX}$ = 1.8 Hz, 1H), 3.32 (ABX, $^2J_{AB}$ = 15.4 Hz, $^3J_{AX}$ = 11.7 Hz, 1H), 3.41 (s, 3H), 3.43 (s, 3H), 4.37 (s, 1H), 5.19 (ABX, $^3J_{AX}$ = 11.7 Hz, $^3J_{BX}$ = 1.8 Hz, 1H), 7.28 (s, 1H), 7.31 (d, J = 8.1 Hz, 2H), 7.59 (d, J = 8.1 Hz, 2H); ^{13}C NMR δ 10.7, 21.9, 23.8, 24.0, 25.9, 36.8, 44.2, 55.28, 55.29, 94.4, 104.9, 105.9, 122.6, 125.1, 125.9, 126.7, 130.5, 135.9, 145.6, 203.2; anal. calcd for $C_{22}H_{29}BrN_2O_7S$: C, 48.44; H, 5.36; N, 5.14%. Found: C, 48.70; H, 5.30; N, 5.17%.

6-(4-Bromo-3-methyl-1*H*-pyrrol-2-yl)-1,1-dimethoxy-4,4-dimethyl-5-nitrohexan-2-one (6-H). Following a general procedure,[50] a sample of **6-Ts** (9.12 g, 16.7 mmol) was treated with TBAF (34 mL, 1.0 M in THF, 34 mmol), and the reaction mixture was stirred for 1 h at reflux. A saturated solution of aqueous $NaHCO_3$ (100 mL) was added followed by ethyl acetate (50 mL). The mixture was extracted with ethyl acetate. The organic layer was dried (Na_2SO_4), concentrated to a

brown oil, dried under high vacuum for 2 h, and chromatographed (silica, CH_2Cl_2) to give a light brown oil (4.00 g, 61%): ^{1}H NMR δ 1.13 (s, 3H), 1.22 (s, 3H), 1.95 (s, 3H), 2.60, 2.70 (AB, ^2J = 18.8 Hz, 2H), 2.99 (ABX, $^2J_{AB}$ = 15.4 Hz, $^3J_{BX}$ = 2.5 Hz, 1H), 3.24 (ABX, $^2J_{AB}$ = 15.4 Hz, $^3J_{AX}$ = 11.8 Hz, 1H), 3.41 (s, 3H), 3.42 (s, 3H), 4.38 (s, 1H), 5.12 (ABX, $^3J_{AX}$ = 11.8 Hz, $^3J_{BX}$ = 2.5 Hz, 1H), 6.59 (s, 1H), 8.29 (br s, 1H); ^{13}C NMR δ 9.8, 24.4, 24.4, 25.6, 36.6, 45.4, 55.39, 55.40, 94.1, 99.0, 104.7, 116.1, 116.7, 122.5, 204.2; ESI-MS obsd 391.0864, calcd 391.0863 [(M + H)$^+$, M = $C_{15}H_{23}BrN_2O_5$].

3,13-Dibromo-5-methoxy-2,8,8,12,18,18-hexamethylbacteriochlorin (MeOBC-MeBr). Following a general procedure,[46] a solution of **1** (675 mg, 1.98 mmol, 18 mM) in anhydrous CH_2Cl_2 (110 mL) was treated first with 2,6-DTBP (3.61 mL, 15.8 mmol, 144 mM) and second with TMSOTf (1.44 mL, 7.92 mmol, 72 mM). The reaction mixture was stirred at room temperature for 16 h. The reaction mixture was concentrated, and the residue was chromatographed [silica, hexanes/CH_2Cl_2 (1 : 1)]. A single green band was collected and concentrated to a green solid (122 mg, 21%): ^{1}H NMR δ –1.99 (br s, 1H), –1.78 (br s, 1H), 1.94 (s, 6H), 1.96 (s, 6H), 3.38 (s, 3H), 3.41 (s, 3H), 4.32 (s, 3H), 4.40 (s, 2H), 4.43 (s, 2H), 8.53 (s, 1H), 8.57 (s, 1H), 8.72 (s, 1H); ^{13}C NMR δ 13.0, 13.2, 31.2, 31.4, 45.9, 46.1, 47.6, 52.0, 64.5, 94.1, 94.4, 95.8, 106.8, 113.0, 125.7, 129.9, 131.8, 132.4, 133.8, 134.9, 160.9; ESI-MS obsd 585.0837, calcd 585.0859 [(M + H)$^+$, M = $C_{27}H_{30}Br_2N_4O$]; λ_{abs} (CH_2Cl_2) 351, 373, 502, 725 nm.

3,13-Dibromo-2,8,8,12,18,18-hexamethylbacteriochlorin (HBC-MeBr). Following a general procedure,[44,46] a solution of **1** (1.36 g, 3.99 mmol, 5 mM) in anhydrous CH_3CN (800 mL) was treated with $BF_3{\cdot}OEt_2$ (4.9 mL, 40 mmol, 50 mM). The reaction mixture was stirred at room temperature for 16 h. Excess TEA (6.0 mL) was added to the reaction mixture. The reaction mixture was concentrated, and the residue was chromatographed [silica, hexanes/CH_2Cl_2 (1 : 1)] to afford a green solid (139 mg, 13%): ^{1}H NMR δ –2.15 (br s, 2H), 1.96 (s, 12H), 3.40 (s, 6H), 4.46 (s, 4H), 8.60 (s, 2H), 8.87 (s, 2H); ESI-MS obsd 555.0745, calcd 555.0753 [(M + H)$^+$, M = $C_{26}H_{28}Br_2N_4$]; λ_{abs} (CH_2Cl_2) 346, 371, 491, 731 nm.

3,13-Diacetyl-5-methoxy-2,8,8,12,18,18-hexamethylbacteriochlorin (MeOBC-MeA). Following a procedure for replacement of a bromo group with an acetyl group on a bacteriochlorin,[45,58] a mixture of **MeOBC-MeBr** (82 mg, 0.14 mmol), tributyl-(1-ethoxyvinyl)tin (195 μL, 0.56 mmol) and $(PPh_3)_2PdCl_2$ (98 mg, 0.14 mmol) was refluxed in THF (14 mL) for 23 h in a Schlenk flask. The reaction mixture was treated with 10% aqueous HCl (40 mL) at room temperature for 10 min. The reaction mixture was poured into a saturated aqueous solution of $NaHCO_3$ and extracted with dichloromethane. The organic layer was dried (Na_2SO_4), concentrated and chromatographed [silica, CH_2Cl_2/EtOAc (99:1)] to give a purple solid (23 mg, 32%): ^{1}H NMR δ –1.84 (br s, 1H), –1.55 (br s, 1H), 1.93 (s, 6H), 1.97 (s, 6H), 2.98 (s, 3H), 3.20 (s, 3H), 3.33 (s, 3H), 3.62 (s, 3H), 4.15 (s, 3H), 4.35 (s, 2H), 4.39 (s, 2H), 8.50 (s, 1H), 8.64 (s, 1H), 9.35 (s, 1H); ESI-MS obsd 513.2857, calcd 513.2860 [(M + H)$^+$, M = $C_{31}H_{36}N_4O_3$]; λ_{abs} (CH_2Cl_2) 362, 523, 743 nm.

3,13-Diacetyl-2,8,8,12,18,18-hexamethylbacteriochlorin (HBC-MeA). Following a procedure for replacement of a bromo group with an acetyl group on a bacteriochlorin,[45,58] a mixture of **HBC-MeBr** (40 mg, 0.072 mmol), tributyl-(1-ethoxyvinyl)tin (100 μL, 0.288 mmol) and $(PPh_3)_2PdCl_2$ (51 mg, 0.072 mmol) was refluxed in THF (7 mL) for 23 h in a Schlenk flask. The reaction mixture was treated with 10% aqueous HCl (40 mL) at room temperature for 10 min. The reaction mixture was poured into a saturated aqueous solution of $NaHCO_3$ and extracted with dichloromethane. The organic layer was dried (Na_2SO_4), concentrated and chromatographed (silica, CH_2Cl_2) to give a purple solid (12 mg, 35%): ^{1}H NMR δ –1.32 (br s, 2H), 1.94 (s, 12H), 3.19 (s, 6H), 3.61 (s, 6H), 4.39 (s, 4H), 8.59 (s, 2H), 9.35 (s, 2H); ESI-MS obsd 483.2755, calcd 483.2755 [(M + H)$^+$, M = $C_{30}H_{34}N_4O_2$]; λ_{abs} (CH_2Cl_2) 359, 389, 523, 766 nm.

3,13-Diacetyl-15-bromo-5-methoxy-2,8,8,12,18,18-hexamethylbacteriochlorin (MeOBC-MeA-Br[15]). A solution of **MeOBC-MeA** (8.0 mg, 0.015 mmol) in THF (6.5 mL) was treated with NBS (2.9 mg, 0.015 mmol, from 0.50 M freshly prepared THF stock solution) at room temperature for 1 h. TLC analysis (silica, CH_2Cl_2) showed the disappearance of starting material and the presence of only one new spot. The reaction mixture was diluted with CH_2Cl_2 and washed with saturated aqueous $NaHCO_3$. The organic layer was dried (Na_2SO_4), concentrated and chromatographed (silica, CH_2Cl_2) to afford a green solid (6.2 mg, 70%): ^{1}H NMR δ –2.09 (br s, 1H), –1.87 (br s, 1H), 1.94 (s, 6H), 1.95 (s, 6H), 2.99 (s, 3H), 3.03 (s, 3H), 3.31 (s, 3H), 3.34 (s, 3H), 4.15 (s, 3H), 4.35 (s, 2H), 4.41 (s, 2H), 8.51 (s, 1H), 8.58 (s, 1H); ESI-MS obsd 512.2782, calcd 512.2782 [(M – Br + H)$^+$, M = $C_{31}H_{35}BrN_4O_3$]; λ_{abs} (CH_2Cl_2) 365, 376, 517, 726 nm.

3,13-Diacetyl-5,15-dibromo-2,8,8,12,18,18-hexamethylbacteriochlorin (BC-MeA-Br[5,15]). A solution of **HBC-MeA** (17 mg, 0.035 mmol) in THF (18 mL) was treated with NBS (6.3 mg, 0.035 mmol, from 0.50 M freshly prepared THF stock solution) at room temperature for 1 h. TLC analysis (silica, CH_2Cl_2) showed unreacted starting material and a new component. The reaction mixture was diluted with CH_2Cl_2 and washed with saturated aqueous $NaHCO_3$. The organic layer was dried (Na_2SO_4), concentrated and chromatographed (silica, CH_2Cl_2). The first band (purple) was the remaining starting bacteriochlorin (4.0 mg) and the second band (green) was the (dibrominated) title compound (5.0 mg, 22%): ^{1}H NMR δ –1.77 (br s, 2H), 1.94 (s, 12H), 3.04 (s, 6H), 3.32 (s, 6H), 4.42 (s, 4H), 8.56 (s, 2H); ESI-MS obsd 638.0887 and 559.1700, calcd 638.0892 and 559.1709 [(M)$^+$ and (M – Br)$^+$, M = $C_{30}H_{32}Br_2N_4O_2$]; λ_{abs} (CH_2Cl_2) 359, 381, 518, 732 nm.

3-Acetyl-5-methoxy-2,8,8,12,18,18-hexamethylbacterio-13^1-oxophorbine (MeOBOP). Following a reported procedure,[53] a mixture of **MeOBC-MeA-Br[15]** (9.0 mg, 0.015 mmol), Cs_2CO_3 (25 mg, 0.077 mmol), and $(PPh_3)_2PdCl_2$ (11 mg, 0.015 mmol) was refluxed in toluene (1.6 mL) for 20 h in a Schlenk flask. The reaction mixture was cooled to room temperature and chromatographed [silica, CH_2Cl_2/THF (99 : 1)] to afford a purple solid (6.6 mg, 86%): ^{1}H NMR δ –1.39 (br s, 1H), 0.12 (br s, 1H), 1.90 (s, 6H), 1.91 (s, 6H), 2.91 (s, 3H), 3.23 (s, 3H), 3.46 (s, 3H), 4.05 (s, 2H), 4.07 (s, 3H), 4.27 (s, 2H),

4.88 (s, 2H), 8.25 (s, 1H), 8.39 (s, 1H); ESI-MS obsd 511.2701, calcd 511.2704 [(M + H)$^+$, M = $C_{31}H_{34}N_4O_3$]; IR (NaCl) ν, cm^{-1} 3435, 2954, 2918, 2850, 1687, 1630, 1360, 1226, 1132, 1084; λ_{abs} (toluene) 359, 372, 530, 733 nm.

15^2-*N*-Benzyl-3-ethoxycarbonyl-2,12-diethyl-5-methoxy-8,8,18,18-tetramethylbacteriochlorin-13,15-dicarboximide (MeOBC-I). Following a reported procedure,[54] a mixture of **MeOBC-EtEs-Br**[15] (7.7 mg, 0.011 mmol), $Pd(PPh_3)_4$ (13 mg, 0.011 mmol), and Cs_2CO_3 (11 mg, 0.034 mmol) was dried under high vacuum in a Schlenk flask for 1 h. The flask was then filled with CO and THF (1.5 mL) containing benzylamine (5 μL, 0.05 mmol) was added. The reaction mixture was then stirred at 80 °C for 20 h under a CO atmosphere. The reaction mixture was cooled to room temperature and chromatographed (silica, CH_2Cl_2) to afford a purple solid (4.8 mg, 62%): ^{1}H NMR δ −0.90 (br s, 1H), −0.43 (br s, 1H), 1.61 (t, J = 7.2 Hz, 3H), 1.73 (m, 6H), 1.87 (s, 6H), 1.90 (s, 6H), 3.73 (q, J = 7.7 Hz, 2H), 4.15–4.28 (q, J = 7.2 Hz, 2H), 4.22 (s, 3H), 4.25 (s, 2H), 4.69 (s, 2H), 4.75 (q, J = 7.2 Hz, 2H), 5.67 (s, 2H), 7.32–7.44 (m, 3H), 7.74 (d, J = 7.4 Hz, 2H), 8.40 (s, 1H), 8.68 (s, 1H); ESI-MS obsd 688.3496, calcd 688.3493 [(M + H)$^+$, M = $C_{41}H_{45}N_5O_5$]; IR (NaCl) ν, cm^{-1} 3435, 3386, 2959, 2919, 1728, 1682, 1647, 1537, 1215, 1149, 1126, 1088; λ_{abs} (toluene) 351, 371, 407, 550, 793 nm.

15-Bromo-3,13-diethoxycarbonyl-2,12-diethyl-8,8,18,18-tetramethylbacteriochlorin (HBC-EtEs-Br[15]**).** A solution of **HBC-EtEs** (50 mg, 0.088 mmol) in THF (35 mL) was treated with NBS (16 mg, 0.088 mmol, from 0.50 M freshly prepared THF stock solution) at room temperature for 1 h. The reaction mixture was diluted with CH_2Cl_2 and washed with saturated aqueous $NaHCO_3$. The organic layer was dried (Na_2SO_4), concentrated and chromatographed (silica, CH_2Cl_2) to afford a green solid (10. mg, 18%): ^{1}H NMR δ −1.61 (br s, 1H), −1.50 (br s, 1H), 1.60 (t, J = 7.2 Hz, 6H), 1.66–1.84 (m, 6H), 1.94 (s, 6H), 1.95 (s, 6H), 3.82 (q, J = 7.7 Hz, 2H), 4.15 (q, J = 7.4 Hz, 2H), 4.41 (s, 2H), 4.43 (s, 2H), 4.77 (m, 4H), 8.58 (s, 1H), 8.64 (s, 1H), 9.63 (s, 1H); ESI-MS obsd 649.2383, calcd 649.2384 [(M + H)$^+$, M = $C_{34}H_{41}BrN_4O_4$]; λ_{abs} (CH_2Cl_2) 354, 380, 520, 748 nm.

15^2-*N*-Benzyl-3-ethoxycarbonyl-2,12-diethyl-8,8,18,18-tetramethylbacteriochlorin-13,15-dicarboximide (HBC-I). Following a reported procedure,[54] a mixture of **HBC-EtEs-Br**[15] (9.7 mg, 0.011 mmol), $Pd(PPh_3)_4$ (17 mg, 0.015 mmol), and Cs_2CO_3 (15 mg, 0.045 mmol) was dried under high vacuum in a Schlenk flask. The flask was then filled with CO and THF (2.0 mL) containing benzylamine (7 μL, 0.06 mmol) was added. The reaction mixture was then stirred at 80 °C for 20 h under a CO atmosphere. The reaction mixture was cooled to room temperature and chromatographed (silica, CH_2Cl_2) to afford a purple solid (4.0 mg, 44%): ^{1}H NMR δ −0.69 (br s, 1H), −0.47 (br s, 1H), 1.71 (m, 9H), 1.90 (s, 6H), 1.92 (s, 6H), 3.99–4.15 (q, J = 7.2 Hz, 2H), 4.16–4.29 (q, J = 7.4 Hz, 2H), 4.33 (s, 2H), 4.72 (s, 2H), 4.77 (q, J = 7.2 Hz, 2H), 5.68 (s, 2H), 7.31–7.44 (m, 3H), 7.70–7.82 (m, 2H), 8.56 (s, 1H), 8.71 (s, 1H), 9.54 (s, 1H); ESI-MS obsd 658.3399, calcd 658.3388 [(M + H)$^+$, M = $C_{40}H_{43}N_5O_4$]; IR (NaCl) ν, cm^{-1} 3431, 2956, 2918, 2848, 1680, 1649, 1423, 1217, 1149, 1095; λ_{abs} (toluene) 359, 408, 544, 818 nm.

II Photophysical measurements

Static absorption and fluorescence measurements were performed as described previously.[69,70] Argon-purged solutions of the samples in toluene with an absorbance of $\leq$0.10 at the excitation wavelength were used for the fluorescence spectral, quantum yield, and lifetime measurements. Fluorescence lifetimes were obtained using a phase modulation technique and Soret-band excitation[70] or *via* decay measurements using Soret-region excitation pulses obtained from a nitrogen-pumped dye laser and time-correlated-single-photon-counting detection. Emission measurements employed 2–4 nm excitation- and detection-monochromator bandwidths and 0.2 nm data intervals. Emission spectra were corrected for detection-system spectral response. Fluorescence quantum yields were determined relative to free base tetraphenylporphyrin (Φ_f = 0.090),[71] chlorophyll *a* in benzene (Φ_f = 0.325)[72] or chlorophyll *a* in toluene (which was found here to have the same value as in benzene).

III Density functional theory calculations

DFT calculations were performed with Spartan '08 for Windows version 1.2.0 in parallel mode[73] on a PC equipped with an Intel i7-975 cpu, 24 GB ram, and three 300 GB, 10k rpm hard drives. The hybrid B3LYP functional and the 6-31G* set were employed. The equilibrium geometries were fully optimized using the default parameters of the Spartan '08 program.

Acknowledgements

This work was supported by grants from the Division of Chemical Sciences, Geosciences and Biosciences Division, Office of Basic Energy Sciences of the U.S. Department of Energy to D.F.B. (DE-FG02-05ER15660), D.H. (DE-FG02-05ER15661) and J.S.L. (DE-FG02-96ER14632). Mass spectra were obtained at the Mass Spectrometry Laboratory for Biotechnology at North Carolina State University. Partial funding for the facility was obtained from the North Carolina Biotechnology Center and the National Science Foundation.

References

1 M. Kobayashi, M. Akiyama, H. Kano and H. Kise, *Chlorophylls and Bacteriochlorophylls: Biochemistry, Biophysics, Functions and Applications*, ed. B. Grimm, R. J. Porra, W. Rüdiger and H. Scheer, Springer, Dordrecht, The Netherlands, 2006, vol. 25, ch. 6, pp. 79–94.
2 M. Wasielewski and W. A. Svec, *J. Org. Chem.*, 1980, **45**, 1969–1974.
3 A. Osuka, S. Marumo, Y. Wada, I. Yamazaki, T. Yamazaki, Y. Shirakawa and Y. Nishimura, *Bull. Chem. Soc. Jpn.*, 1995, **68**, 2909–2915.
4 T. Miyatake, H. Tamiaki, A. R. Holzwarth and K. Schaffner, *Photochem. Photobiol.*, 1999, **69**, 448–456.
5 H. Mössler, M. Wittenberg, D. Niethammer, R. K. Mudrassagam, H. Kurreck and M. Huber, *Magn. Reson. Chem.*, 2000, **38**, 67–84.
6 M. A. Grin, I. S. Lonin, S. V. Fedyunin, A. G. Tsiprovskiy, A. A. Strizhakov, A. A. Tsygankov, A. A. Krasnovsky and A. F. Mironov, *Mendeleev Commun.*, 2007, **17**, 209–211.

7 C. Muthiah, M. Taniguchi, H.-J. Kim, I. Schmidt, H. L. Kee, D. Holten, D. F. Bocian and J. S. Lindsey, *Photochem. Photobiol.*, 2007, **83**, 1513–1528.
8 J. R. Stromberg, A. Marton, H. L. Kee, C. Kirmaier, J. R. Diers, C. Muthiah, M. Taniguchi, J. S. Lindsey, D. F. Bocian, G. J. Meyer and D. Holten, *J. Phys. Chem. C*, 2007, **111**, 15464–15478.
9 C. Muthiah, H. L. Kee, J. R. Diers, D. Fan, M. Ptaszek, D. F. Bocian, D. Holten and J. S. Lindsey, *Photochem. Photobiol.*, 2008, **84**, 786–801.
10 J. J. Schuitmaker, J. A. van Best, J. L. van Delft, T. M. A. R. Dubbelman, J. A. Oosterhuis and D. de Wolff-Rouendaal, *Invest. Ophthalmol. Visual Sci.*, 1990, **31**, 1444–1450.
11 J. P. Rovers, M. L. de Jode, H. Rezzoug and M. F. Grahn, *Photochem. Photobiol.*, 2000, **72**, 358–364.
12 Y. Chen, A. Graham, W. Potter, J. Morgan, L. Vaughan, D. A. Bellnier, B. W. Henderson, A. Oseroff, T. J. Dougherty and R. K. Pandey, *J. Med. Chem.*, 2002, **45**, 255–258.
13 Y. Chen, G. Li and R. K. Pandey, *Curr. Org. Chem.*, 2004, **8**, 1105–1134.
14 F. H. van Duijnhoven, J. P. Rovers, K. Engelmann, Z. Krajina, S. F. Purkiss, F. A. Zoetmulder, T. J. Vogl and O. T. Terpstra, *Ann. Surg. Oncol.*, 2005, **12**, 808–816.
15 A. S. Brandis, Y. Salomon and A. Scherz, *Chlorophylls and Bacteriochlorophylls: Biochemistry, Biophysics, Functions and Applications*, ed. B. Grimm, R. J. Porra, W. Rüdiger and H. Scheer, Springer, Dordrecht, The Netherlands, 2006, vol. 25, ch. 33, pp. 485–494.
16 A. L. Gryshuk, Y. Chen, W. Potter, T. Ohulchansky, A. Oseroff and R. K. Pandey, *J. Med. Chem.*, 2006, **49**, 1874–1881.
17 S. Fukuzumi, K. Ohkubo, X. Zheng, Y. Chen, R. K. Pandey, R. Zhan and K. M. Kadish, *J. Phys. Chem. B*, 2008, **112**, 2738–2746.
18 M. A. Grin, A. F. Mironov and A. A. Shtil, *Anti-Cancer Agents Med. Chem.*, 2008, **8**, 683–697.
19 M. M. Pereira, C. J. P. Monteiro, A. V. C. Somões, S. M. A. Pinto, L. G. Arnaut, G. F. F. Sá, E. F. F. Silva, L. B. Rocha, S. Simões and S. J. Formosinho, *J. Porphyrins Phthalocyanines*, 2009, **13**, 567–573.
20 E. F. F. Silva, C. Serpa, J. M. Dabrowski, C. J. P. Monteiro, S. J. Formosinho, G. Stochel, K. Urbanska, S. Simões, M. M. Pereira and L. G. Arnaut, *Chem.–Eur. J.*, 2010, **16**, 9273–9286.
21 P. Mroz, Y.-Y. Huang, A. Szokalska, T. Zhiyentayev, S. Janjua, A.-P. Nifli, M. E. Sherwood, C. Ruzié, K. E. Borbas, D. Fan, M. Krayer, T. Balasubramanian, E. Yang, H. L. Kee, C. Kirmaier, J. R. Diers, D. F. Bocian, D. Holten, J. S. Lindsey and M. R. Hamblin, *FASEB J.*, 2010, **24**, 3160–3170.
22 Y.-Y. Huang, P. Mroz, T. Zhiyentayev, T. Balasubramanian, C. Ruzié, M. Krayer, D. Fan, K. E. Borbas, E. Yang, H. L. Kee, C. Kirmaier, J. R. Diers, D. F. Bocian, D. Holten, J. S. Lindsey and M. R. Hamblin, *J. Med. Chem.*, 2010, **53**, 4018–4027.
23 L. Huang, Y.-Y. Huang, P. Mroz, G. P. Tegos, T. Zhiyentayev, S. K. Sharma, Z. Lu, T. Balasubramanian, M. Krayer, C. Ruzié, E. Yang, H. L. Kee, C. Kirmaier, J. R. Diers, D. F. Bocian, D. Holten, J. S. Lindsey and M. R. Hamblin, *Antimicrob. Agents Chemother.*, 2010, **54**, 3834–3841.
24 J. M. Sutton, O. J. Clarke, N. Fernandez and R. W. Boyle, *Bioconjugate Chem.*, 2002, **13**, 249–263.
25 H. L. Kee, R. Nothdurft, C. Muthiah, J. R. Diers, D. Fan, M. Ptaszek, D. F. Bocian, J. S. Lindsey, J. P. Culver and D. Holten, *Photochem. Photobiol.*, 2008, **84**, 1061–1072.
26 H. L. Kee, J. R. Diers, M. Ptaszek, C. Muthiah, D. Fan, J. S. Lindsey, D. F. Bocian and D. Holten, *Photochem. Photobiol.*, 2009, **85**, 909–920.
27 (*a*) S. C. De Rosa, J. M. Brenchley and M. Roederer, *Nat. Med. (N. Y.)*, 2003, **9**, 112–117; (*b*) S. P. Perfetto, P. K. Chattopadhyay and M. Roederer, *Nat. Rev. Immunol.*, 2004, **4**, 648–655; (*c*) P. K. Chattopadhyay, D. A. Price, T. F. Harper, M. R. Betts, J. Yu, E. Gostick, S. P. Perfetto, P. Goepfert, R. A. Koup, S. C. De Rosa, M. P. Bruchez and M. Roederer, *Nat. Med. (N. Y.)*, 2006, **12**, 972–977.
28 H. Scheer, *Chlorophylls and Bacteriochlorophylls: Biochemistry, Biophysics, Functions and Applications*, ed. B. Grimm, R. J. Porra, W. Rüdiger and H. Scheer, Springer, Dordrecht, The Netherlands, 2006, vol. 25, ch. 1, pp. 1–26.
29 H. Tamiaki, M. Kouraba, K. Takeda, S.-I. Kondo and R. Tanikaga, *Tetrahedron: Asymmetry*, 1998, **9**, 2101–2111.
30 S.-I. Sasaki and H. J. Tamiaki, *J. Org. Chem.*, 2006, **71**, 2648–2654.
31 A. N. Kozyrev, G. Zheng, C. Zhu, T. J. Dougherty, K. M. Smith and R. K. Pandey, *Tetrahedron Lett.*, 1996, **37**, 6431–6434.
32 A. F. Mironov, M. A. Grin and A. G. Tsyprovskiy, *J. Porphyrins Phthalocyanines*, 2002, **6**, 358–361.
33 A. F. Mironov, M. A. Grin, A. G. Tsiprovskiy, V. V. Kachala, T. A. Karmakova, A. D. Plyutinskaya and R. I. Yakubovskaya, *J. Porphyrins Phthalocyanines*, 2003, **7**, 725–730.
34 A. F. Mironov, M. A. Grin, A. G. Tsiprovskii, A. V. Segenevich, D. V. Dzardanov, K. V. Golovin, A. A. Tsygnkov and Y. K. Shim, *Russ. J. Bioorg. Chem.*, 2003, **29**, 190–197.
35 A. F. Mironov, M. A. Grin, A. G. Tsiprovskii, R. A. Titeev, E. A. Nizhnik and I. S. Lonin, *Mendeleev Commun.*, 2004, **14**, 204–207.
36 A. N. Kozyrev, Y. Chen, L. N. Goswami, W. A. Tabaczynski and R. K. Pandey, *J. Org. Chem.*, 2006, **71**, 1949–1960.
37 L. N. Goswami, Y. Chen, J. Missert, G. Li, A. Pallenberg and R. K. Pandey, *Heterocycles*, 2007, **71**, 1929–1949.
38 M. A. Grin, I. S. Lonin, A. A. Lakhina, E. S. Ol'shanskaya, A. I. Makaraov, Y. L. Sebyakin, L. Y. Guryeva, P. V. Toukach, A. S. Kononikhin, V. A. Kuzmin and A. F. Mironov, *J. Porphyrins Phthalocyanines*, 2009, **13**, 336–345.
39 S. Fox and R. W. Boyle, *Tetrahedron*, 2006, **62**, 10039–10054.
40 (*a*) T. D. Lash, *J. Porphyrins Phthalocyanines*, 2001, **5**, 267–288; (*b*) B. E. Smith and T. D. Lash, *Tetrahedron*, 2010, **66**, 4413–4422.
41 Y. Vakrat-Haglili, L. Weiner, V. Brumfeld, A. Brandis, Y. Salomon, B. McIlroy, B. C. Wilson, A. Pawlak, M. Rozanowska, T. Sarna and A. Scherz, *J. Am. Chem. Soc.*, 2005, **127**, 6487–6497.
42 L. Limantara, P. Koehler, B. Wilhelm, R. J. Porra and H. Scheer, *Photochem. Photobiol.*, 2006, **82**, 770–780.
43 M. Galezowski and D. T. Gryko, *Curr. Org. Chem.*, 2007, **11**, 1310–1338.
44 H.-J. Kim and J. S. Lindsey, *J. Org. Chem.*, 2005, **70**, 5475–5486.
45 M. Taniguchi, D. L. Cramer, A. D. Bhise, H. L. Kee, D. F. Bocian, D. Holten and J. S. Lindsey, *New J. Chem.*, 2008, **32**, 947–958.
46 M. Krayer, M. Ptaszek, H.-J. Kim, K. R. Meneely, D. Fan, K. Secor and J. S. Lindsey, *J. Org. Chem.*, 2010, **75**, 1016–1039.
47 D. Fan, M. Taniguchi and J. S. Lindsey, *J. Org. Chem.*, 2007, **72**, 5350–5357.
48 K. E. Borbas, C. Ruzié and J. S. Lindsey, *Org. Lett.*, 2008, **10**, 1931–1934.
49 C. Ruzié, M. Krayer, T. Balasubramanian and J. S. Lindsey, *J. Org. Chem.*, 2008, **73**, 5806–5820.
50 M. Krayer, T. Balasubramanian, C. Ruzié, M. Ptaszek, D. L. Cramer, M. Taniguchi and J. S. Lindsey, *J. Porphyrins Phthalocyanines*, 2009, **13**, 1098–1110.
51 C. Ruzié, M. Krayer and J. S. Lindsey, *Org. Lett.*, 2009, **11**, 1761–1764.
52 Nomenclature of bacteriochlorin macrocycles is not fully settled. We here introduce the terminology bacterio-13^1-oxophorbine for the annulated bacteriochlorin by analogy with the accepted nomenclature for the corresponding 13^1-oxophorbine skeleton of chlorophylls. G. P. Moss, *Pure Appl. Chem.*, 1987, **59**, 779–832.
53 J. K. Laha, C. Muthiah, M. Taniguchi and J. S. Lindsey, *J. Org. Chem.*, 2006, **71**, 7049–7052.
54 M. Ptaszek, D. Lahaye, M. Krayer, C. Muthiah and J. S. Lindsey, *J. Org. Chem.*, 2010, **75**, 1659–1673.
55 (*a*) H. Muratake and M. Natsume, *Tetrahedron Lett.*, 1997, **38**, 7581–7582; (*b*) H. Muratake, M. Natsume and H. Nakai, *Tetrahedron*, 2004, **60**, 11783–11803.
56 R. K. Pandey, N. Jagerovic, J. M. Ryan, T. J. Dougherty and K. M. Smith, *Tetrahedron*, 1996, **52**, 5349.
57 (*a*) F. Bellamy, P. Martz and J. Streith, *Heterocycles*, 1975, **3**, 395–400; (*b*) F. Bellamy and J. Streith, *J. Chem. Res., Synop.*, 1979, 18–19.
58 M. Kosugi, T. Sumiya, Y. Obara, M. Suzuki, H. Sano and T. Migita, *Bull. Chem. Soc. Jpn.*, 1987, **60**, 767–768.
59 O. Mass, M. Taniguchi, M. Ptaszek, J. W. Springer, K. M. Faries, J. R. Diers, D. F. Bocian, D. Holten and J. S. Lindsey, *New J. Chem.*, 2011, **35**, 76–88.

60 J. Helaja, A. Y. Tauber, Y. Abel, N. V. Tkachenko, H. Lemmetyinen, I. Kilpeläinen and P. H. Hynninen, *J. Chem. Soc., Perkin Trans. 1*, 1999, 2403–2408.
61 M. Kunieda and H. Tamiaki, *J. Org. Chem.*, 2005, **70**, 820–828.
62 (*a*) H. Tamiaki, M. Amakawa, Y. Shimono, R. Tanikaga, A. R. Holzwarth and K. Schaffner, *Photochem. Photobiol.*, 1996, **63**, 92–99; (*b*) H. Tamiaki, S. Yagai and T. Miyatake, *Bioorg. Med. Chem.*, 1998, **6**, 2171–2178; (*c*) H. Tamiaki, M. Amakawa, A. R. Holzwarth and K. Schaffner, *Photosynth. Res.*, 2002, **71**, 59–67; (*d*) H. Morishita and H. Tamiaki, *Tetrahedron*, 2005, **61**, 6097–6107; (*e*) H. Tamiaki, H. Kitamoto, T. Watanabea and R. Shibata, *Photochem. Photobiol.*, 2005, **81**, 170–176; (*f*) R. Shibata, T. Mizoguchi, T. Inazu and H. Tamiaki, *Photochem. Photobiol. Sci.*, 2007, **6**, 749–757; (*g*) S. Sasaki, K. Mizutani, M. Kunieda and H. Tamiaki, *Tetrahedron Lett.*, 2008, **49**, 4113–4115; (*h*) H. Morishita and H. Tamiaki, *Spectrochim. Acta, Part A*, 2009, **72**, 274–279.
63 M. Kunieda and H. Tamiaki, *Eur. J. Org. Chem.*, 2006, 2352–2361.
64 J. H. C. Smith and A. Benitez, *Modern Methods of Plant Analysis*, ed. K. Paech and M. V. Tracey, Springer-Verlag, Berlin, 1955, vol. IV, pp. 142–196.
65 D. Holten, M. Gouterman, W. W. Parson, M. W. Windsor and M. G. Rockley, *Photochem. Photobiol.*, 1976, **23**, 415–423.
66 M. Gouterman, *The Porphyrins*, ed. D. Dolphin, Academic Press, New York, 1978, vol. 3, pp. 1–165.
67 M. Gouterman, *J. Mol. Spectrosc.*, 1961, **6**, 138–163.
68 W. Wang and Y. Kishi, *Org. Lett.*, 1999, **1**, 1129–1132.
69 F. Li, S. Gentemann, W. A. Kalsbeck, J. Seth, J. S. Lindsey, D. Holten and D. F. Bocian, *J. Mater. Chem.*, 1997, **7**, 1245–1262.
70 H. L. Kee, C. Kirmaier, L. Yu, P. Thamyongkit, W. J. Youngblood, M. E. Calder, L. Ramos, B. C. Noll, D. F. Bocian, W. R. Scheidt, R. R. Birge, J. S. Lindsey and D. Holten, *J. Phys. Chem. B*, 2005, **109**, 20433–20443.
71 A. T. Gradyushko, A. N. Sevchenko, K. N. Solovyov and M. P. Tsvirko, *Photochem. Photobiol.*, 1970, **11**, 387–400.
72 G. Weber and F. W. J. Teale, *Trans. Faraday Soc.*, 1957, **53**, 646–655.
73 Except for molecular mechanics and semi-empirical models, the calculation methods used in Spartan have been documented in Y. Shao, L. F. Molnar, Y. Jung, J. Kussmann, C. Ochsenfeld, S. T. Brown, A. T. B. Gilbert, L. V. Slipchenko, S. V. Levchenko, D. P. O'Neill, R. A. DiStasio, Jr., R. C. Lochan, T. Wang, G. J. O. Beran, N. A. Besley, J. M. Herbert, C. Y. Lin, T. Van Voorhis, S. H. Chien, A. Sodt, R. P. Steele, V. A. Rassolov, P. E. Maslen, P. P. Korambath, R. D. Adamson, B. Austin, J. Baker, E. F. C. Byrd, H. Dachsel, R. J. Doerksen, A. Dreuw, B. D. Dunietz, A. D. Dutoi, T. R. Furlani, S. R. Gwaltney, A. Heyden, S. Hirata, C.-P. Hsu, G. Kedziora, R. Z. Khalliulin, P. Klunzinger, A. M. Lee, M. S. Lee, W.-Z. Liang, I. Lotan, N. Nair, B. Peters, E. I. Proynov, P. A. Pieniazek, Y. M. Rhee, J. Ritchie, E. Rosta, C. D. Sherrill, A. C. Simmonett, J. E. Subotnik, H. L. Woodcock III, W. Zhang, A. T. Bell, A. K. Chakraborty, D. M. Chipman, F. J. Keil, A. Warshel, W. J. Hehre, H. F. Schaefer III, J. Kong, A. I. Krylov, P. M. W. Gill and M. Head-Gordon, *Phys. Chem. Chem. Phys.*, 2006, **8**, 3172–3191.